NTNU

Norwegian University of
Science and Technology

Automated classification and quantification of spatio-temporal parameters in cross-country skiing skating technique by analysis of inertial sensor data and sensor insole data

Lene-Kristine Garsjø

Master of Science in Cybernetics and Robotics
Submission date: February 2017
Supervisor: Øyvind Stavdahl, ITK
Co-supervisor: Øyvind Sandbakk, INM
Jan Kocbach, INM

Norwegian University of Science and Technology
Department of Engineering Cybernetics

Acknowledgment

A special thanks to my main supervisor at the Norwegian University of Science and Technology (NTNU), associate professor Øyvind Stavdahl, for positive and great guidance, and the opportunity to study this project. I would like to thank my co-supervisors at SenTIF Jan Kocbach and Øyvind Sandbakk for consistent and exceptional guidance.

I am very grateful for the proofreading sister-in-law Gry Almdahl, who voluntarily proofread this thesis while working full time. Last but not the least, I would like to thank my family: my parents and my brother for supporting me throughout my entire education. I am also grateful for the for the patience and support from my life partner while finalizing this thesis.

Abstract

The aim of this thesis was (1) to develop a method for dividing cross-country skiing cycles into phases, and (2) extract and select features characterizing the change in center of pressure (CoP) during these phases. Both tasks were solved by the help of Moticon OpenGo insole data (pressure sensors + accelerometer) from athletes on different skill levels. The accelerometer data produced extremal values which could be detected by an algorithm. The different phases were identified through combining search areas (based on total foot pressure) with the extremal points from accelerometer data. Selected features were compared between subjects in order to reveal whether or not they could differentiate between subjects on different skill levels. Analysis of the foot movement in cross-country skiing could facilitate a more accurate understanding of the athletes' techniques, which might facilitate a better performance.

This study showed that it was possible to divide cycles into phases by the use of Moticon's OpenGo insole data. The calculated phase-features indicated that features of athletes on the same skill level had more in common than features of athletes on different skill levels. One of the main results was that elite athletes spent a larger percentage of their cycle time on the gliding phase, than athletes on lower skill levels. Another result was that features describing the change of CoP during the gliding phase could classify five out of six athletes correctly according to skill level.

Abbreviations

IMU	=	Inertial measurement unit
G2	=	Paddle dance
G3	=	Double dance
G4	=	Single dance
Peak force	=	Highest force value inside a cycle
CT	=	Cycle time, duration of a full cycle
CR	=	Cycle rate, number of cycles within a time unit, e.g. cycles / second
Elite level	=	Athletes competing nationally and internationally
Intermediate level	=	Athletes competing on district level
PCA	=	Principal component analysis

Contents

Chapter 1

Introduction

The introduction chapter includes some paragraphs taken from *Automated movement based classification of techniques in classic cross-country skiing* [Garsjø, 2016]. This is because the reasoning and the main background for performing this study is the same as the earlier project by the same author.

Modern instrumentation allows studies of human movement at an unprecedented level of detail in a vast number of contexts. The long-term aim of the project this thesis is a part of, is to exploit this potential in order to study, describe and eventually improve techniques and exercise regimens in top-level cross-country skiing. The movement patterns in the cross-country skiing skating technique are cyclic, and each subtechnique can be divided into cycles, which in turn can be divided into different phases. The four major subtechniques within the skating technique are G2 (paddling), G3 (double dance), G4 (single dance) and G5 (skating without poling). The movement pattern within each cycle in each of the subtechniques can be divided into distinct phases (see figure 1.1 for a visual overview) which can be described by spatio-temporal variables. These variables include the length of the gliding phase, the length of the poling phase and the length of the kick phase. Analysis of the different phases coupled with velocity and time gains in both competition and training, provides important information, which can help improve the understanding of a wide range of performance related topics within cross-country skiing. The methods developed for analysing movement patterns in cross-country skiing may also be relevant in the classification of other movement patterns, e.g. classifying different walking and running styles. Although the current thesis has relevance mainly for cross-

country skiers, the method developed may have implications for many populations and clinical settings.

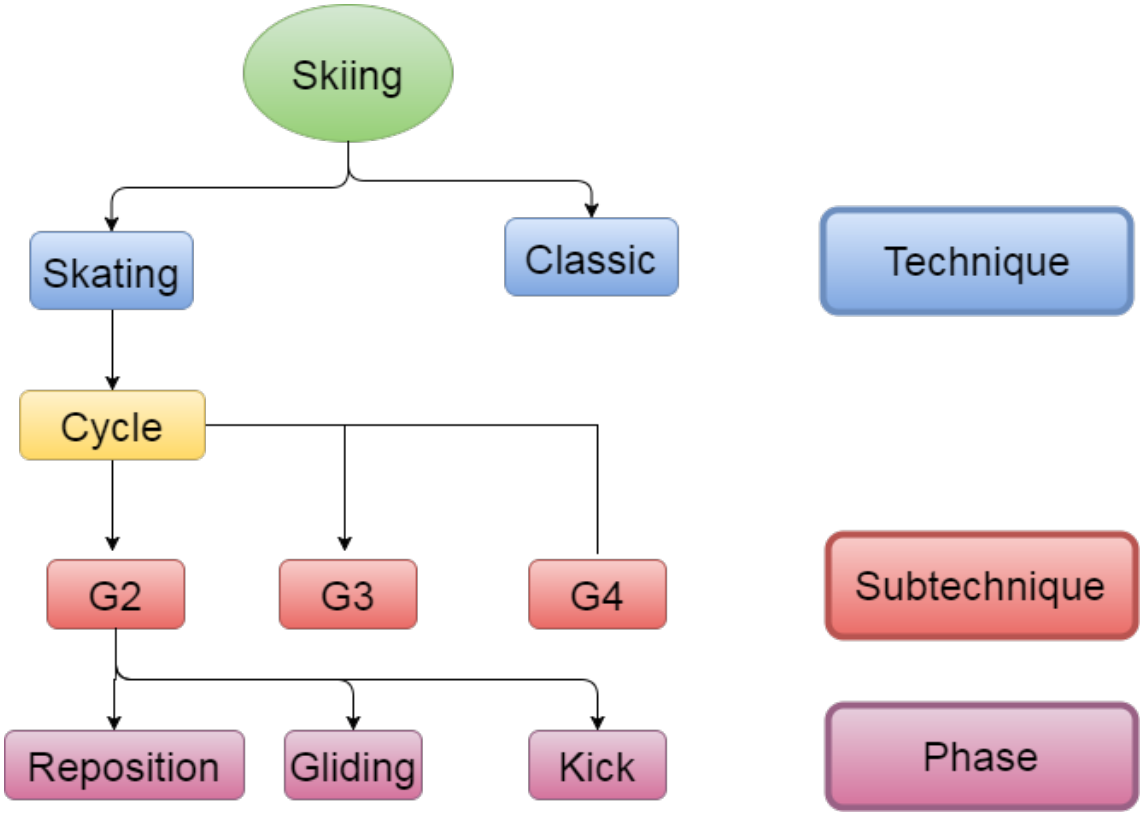

Figure 1.1: Cross-country skiing phrases

1.1 Background

This thesis is part of a research study at the Center for Elite Sports Research (SenTIF) - NTNU, called "Optimization of technique, physical capacity and training in the world's best cross-country skiers, biathletes, Nordic combined athletes and cyclists". Together, SenTIF and the cybernetics department at NTNU aim to develop an automated classification of the subtechniques within cross-country skiing and investigate the possibilities pressure insoles provide when investigating the different phases of a skating subtechnique cycle.

Originally, two student projects were developed, one classified subtechniques within classic cross-country skiing ([Garsjø, 2016]), the other one within the skating technique ([Meland, 2016]). Both projects concluded with the need for more research, which led

to the construction of two new master thesis. One thesis continued the work on classification of subtechniques within classic and skating cross-country skiing. The other thesis investigating the different phases of skating cycles.

1.2 Objective

The objective of the present thesis is to develop a valid method for (1) dividing a cycle into phases and (2) calculating the time spent on each phase based on data from insoles with integrated pressure sensors and Inertial Measurement Unit (IMU). A secondary objective for the project is to extract and calculate features which characterize the change in center of pressure (CoP) during the different phases (minimum during gliding phase) based on insole sensor data. These parameters will be compared because subjects to illustrate whether they can differentiate between subjects on different skill levels.

The algorithms should aim at being robust and work inn all cases without the need for separate calibration for different skiers or for different velocities. The project will study the subtechniques G2, G3 and G4. However, based on initial results on subtechnique may gain the main focus. Cycle and classification is not an included topic in the current project, as this can be done either manually or by algorithms developed in other projects. The objectives can be summarized as:

1. Divide a cycle into phases and calculate the time for each phase based on insole data (pressure sensors) and IMU data.

2. Extract and calculate features which characterize the change in CoP during the different phases (minimum during gliding phase) based on insole sensor data.

3. Compare the above mentioned features between subjects to illustrate wheter they can differentiate between subjects on different skill levels.

1.3 Personal interpretation

In order to answer the objectives in this thesis I first needed to define the different phases of a cycle. The predefined phases given in the introduction (gliding phase, poling phase

and kick phase) have a duration relative to the ski poles' ground contact which may not be detectable in this study. Consequently, further investigation was necessary in order to decide which phases were to be included in the project. Phases described in sport specific literature were studied and compared to our own initial data results. Based on this the cycles were divided into phases. The defined conditions had to be regonizable in a video (100 Hz) of an athlete performing the different subtechniques.

With the phases defined, the algorithms were to be developed. The algorithm should analyse data from the pressure sensor and the integrated accelerometer and use this information in order to divide the phases. If the initial results showed that both legs performed the same movement, algorithm analyzes of one foot only would be sufficient. The change in CoP should be investigated during the gliding phase at a minimum. To what extent specific features could give information about the skill level of an athlete would also be evaluated. The relevant features were compared among athletes on different skill levels for verification. Due to the design of this thesis (a limited number of subjects included), statistically significant results could not be achieved. Further research is recommended.

1.4 Methodology

The data this thesis is primarily based on were obtained in Granåsen, Trondheim, Norway October 2016. Six different athletes were studied, three of which were on an elite level and three on an intermediate level. They performed a set protocol containing the different subtechniques G2, G3 and G4, on an indoor treadmill, wearing Moticon's OpenGo insoles in their own shoes. A new data collection was arranged in November 2016, with recordings from snow conditions. This collection took place in Granåsen, Trondheim, with the same equipment as in the earlier data collection, but with only one athlete. This athlete was on an elite level.

Moticon's OpenGo insoles contain pressure sensors, and an integrated accelerometer. As described on Moticon's website [Moticon, 2017], the accelerometer in the OpenGo insoles has the Z-axis pointing normal to the reference ground plane, the Y-axis in the line of walking (anterior) and the X-axis in medial/lateral direction. The subjects were all familiar with roller skiing on a treadmill. All skiers were fully acquainted with the

nature of the study before they gave their written informed consent to participate.

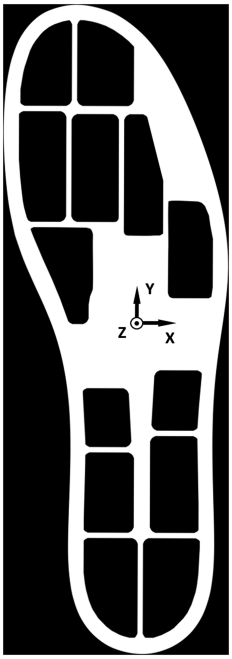

Figure 1.2: Moticon OpenGo insoles accelerometer axis

All data collected has been analyzed mainly by Matlab. The data was throughout the process analyzed by a single-side frequency spectrum with logarithmic scale in Matlab, in order to determine the information level before it was filtered. The intention was to minimize the amount of noise and, at the same time ensure that there was no loss of information. All video analysis has been done by using VLC media player and MPC-HC (Classic media player). In order to visualize some computations and results, the multivariate data analysis program Unscrambler was used.

The phases were initially identified visually, and later determined by distinct physical movements shown in the accelerometer data. The phase detection problem was solved by using a specific set of conditions for each phase, and the apriori knowledge of the order of which the phases appear within a cycle. The characteristics of the CoP-change were found by trend analyses. Classification of athletes into the elite or intermediate groups were based on the calculated characteristics. The flow of the computations are shown in figure 1.3.

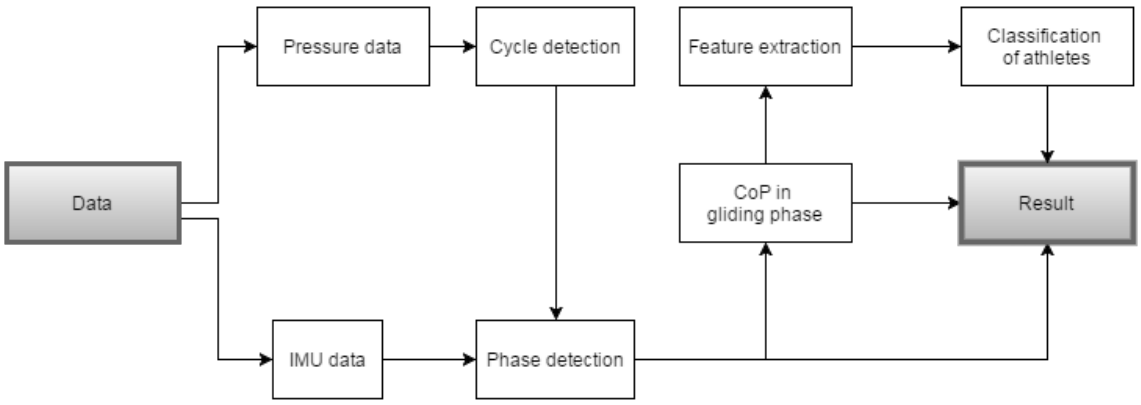

Figure 1.3: The flow of computations

1.5 Structure and contribution

Following this introduction is a chapter explaining the methods used in the project in order to solve the objectives defined above. The methods will be introduced in the order of which they appeared. In chapter 3, the main results will be presented, followed by a discussion in chapter 4. A conclusion is provided in chapter 5. The thesis' main contributions are:

1. Phase detection algorithm
2. Analysis of CoP change during the gliding phase and the kick phase
3. Parameters (including time spent in each phase) which describe the different phases
4. Features which describe the CoP change during the gliding phase
5. Features which distinguish between athletes on different skill levels

1.6 Previous research

Multiple different studies with sensor equipment have previously been done of cross country skiing athletes. The earliest studies measured angles and forces in poles and legs through force plates and body markers, but the studies are now trending to use more wearable technology. This gives less complex data recordings and many possibilities like recording data outside of a lab environment.

1.6.1 IMU used in classification of subtechniques

Inertial measurement unit technology has shown to be very useful in analyzing kinematic movement without the limitation of restricted capture volume. It also has the benefit of low time costs for the measurement preparation and data analysis ([Krüger and Edelmann-Nusser, 2010]).

A study showed that the different subtechniques in skating and classic skiing, visually could be classified by data from one IMU located on the upper back ([Marsland et al., 2012]). Another study observed that it was possible to distinguish first gear (V1) and second gear (V2) in skating cross-country skiing by using acceleration data from five different sensors placed around the hip area of an athlete ([Myklebust et al., 2014]).

These studies showed that it is possible to detect different skiing subtechniques by the use of IMU-data. Automatic classification systems of subtechniques have been built in several studies ([Stöggl et al., 2014], [Sakurai et al., 2014], [Sakurai et al., 2016]), and these have been successful in identifying subtechniques.

Classification challenges in cross-country skiing can be compared to those of movement patterns within other fields of study. As study analyzing acceleration data from a sensor mounted on the body, showed that detection of human steps was possible ([Våga, 2008]). The overall objective was to detect steps in humans with an abnormal movement pattern, which could in turn cohere to detecting a specific technique for different athletes.

1.6.2 Pressure insoles in cross-country research

Pressure insoles have been used in cross-country studies for the past 10 years (table 1.1), in order to get more information about bio-mechanical features. Most of the studies have been performed with Pedar insoles system ([Novel.de, 2017]). The studies have mostly investigated the forces in shoes and poles, and the relationship between them (e.g. article [Holmberg, 2005]). The different forces applied to the shoes in different speeds and in different subtechniques have been another subject of investigation (e.g. article [Andersson, 2013]).

The Moticon sensor insoles ([Moticon, 2017]) used in our own thesis have previously been validated by others [Stggl and Martiner, 2017]. They concluded that the OpenGo could be applied in both clinical and research settings for the purpose of evaluating tem-

Table 1.1: A collection of articles that use Pedar insole system

Work	Sub-Technique	Summary
[Holmberg, 2005]	Poling	-Pole and plantar ground reaction forces -Joint angles (elbow, hip, knee, and ankle) -Cycle characteristics -Electromyography (EMG)
[Lindinger, 2009]	Uphill diagonal	-Pole and leg kinematics -Identifies biomechanical factors related to performance
[Lindinger SJ, 2009]	Double poll	-Investigates how elite skiers control DP speed-Cycle characteristics -Pole/plantar forces Elbow/hip/knee angles
[Stöggl T, 2010]	Skating	-To compare the double-push skating technique with the V2 and the V1 -To provide kinetic and kinematic data of the V1 -To test the hypothesis that the double-push skating technique is faster compared with the V2 and the V1 skating techniques.
[Stöggl, 2009]	Skating (V2), poling & diagonal stride	-Relationships between general strength, maximal skiing speed, pole and leg kinetics and kinematics.
[Stöggl and Lindinger, 2008]	Skating ("double-push")	-Investigates double-push skating technique -Pole/Plantar force -Knee angle -Cycle characteristics -Electromyography
[Levy, 2011]	Double poll with kick	-Joint kinematics -Pole/plantar forces
[Andersson, 2013]	Diagonal stride	-Cycle and force characteristics
[Andersson, 2014]	Herringbone	-Analyzes the kinematics and kinetics
[Stöggl, 2014]	Skating (V1, high speed)	-Detailed kinetics and kinematics -Identifies factors that predict performance.
[Andersson, 2016]	Diagonal & herringbone	-Global navigation system + video analysis -The effects of an increasing velocity
[Göpfert, 2013]	Double poll with kick	- Phase definition - Speed adaptation mechanisms

poral, force and balance parameters during different types of motion. The main weakness found was the medio-lateral CoP measurement, whereas anterior-posterior CoP had a higher correlation to the reference system (AMTI force-plate system). The Moticon OpenGo insoles combine a pressure insole system and an IMU connected to the soles. Since the separate systems have shown promising results, the combination given in the OpenGo insoles should be a good fit for the objective of our thesis as long as the reported imprecise medio-lateral CoP is accounted for.

1.6.3 Phase definitions

In previously literature there are several different phase definitions. The phase definitions usually start with the differentiation of the duration of ground time for skis and poles before a more detailed differentiation is described. Phases are sometimes defined by the

leg/pole force and joint angles measured [Lindinger, 2009]. Phase definitions of a diagonal classic skiing (DIA) cycle are shown in figure 1.4. Similar phase definitions (angle+force measures) can be found in multiple studies [Andersson, 2013], [Göpfert, 2013], [Holmberg, 2005], [Andersson, 2014] and [Stöggl, 2014]. Other scientists have used total foot force [Stöggl, 2009] and the percent of body weight inflicted upon one shoe as a way of defining the phase of a DIA cycle [Alyse L. Kehler and Kram, 2014] (see figure 1.5).

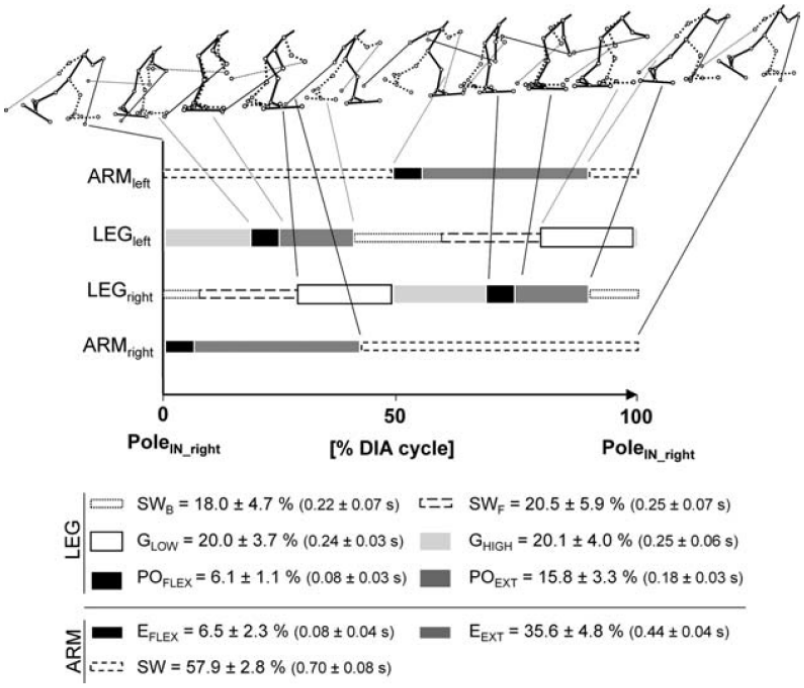

Figure 1. Cycle phase structure and relative (% CT) and absolute (s) phase times during uphill diagonal roller skiing (9°; 11 km/h). The data are mean ± *s*. DIA = diagonal skiing; $Pole_{IN\_right}$ = plant of right pole; SW_B = backward leg swing; SW_F = forward leg swing; G_{LOW} = initial gliding phase in low position; G_{HIGH} = second gliding phase with leg joint extension; PO_{FLEX} = leg push-off flexion; PO_{EXT} = leg push-off extension; E_{FLEX} = elbow flexion; E_{EXT} = elbow extension; SW = arm swing.

Figure 1.4: Figure illustration one DIA cycle definition [Alyse L. Kehler and Kram, 2014]

The following phases have previously been defined for G2 [Myklebust, 2016]:

Kick phase: period between pole and ski liftoffs

Pure gliding phase: period of time ground contact is made by one ski only

Poling phase: period of time ground contact is made by the pole

Reposition time: duration of period without ground contact for pole or ski, respectively

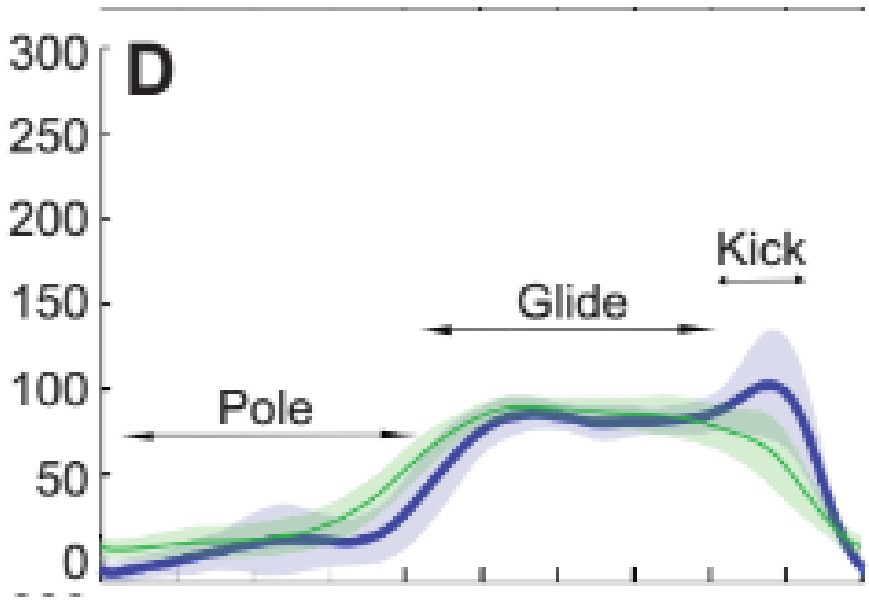

Figure 1.5: Figure illustrating the total force in each phase [Alyse L. Kehler and Kram, 2014]. Y-axis = force, X-axis = time

These phases were detected by IMU and force measurements in poles and skies. The phases were defined by the poles' and skis' ground contact time which ensured very precise phase definitions. Literature studies show, that there are several ways to differentiate between the phases.

Chapter 2

Methods

2.1 Data collection

The treadmill data was obtained in Granåsen, Trondheim, Norway October 2016. Six different athletes were studied: three athletes on an elite level and three athletes on an intermediate level. They performed a set protocol containing the different subtechniques G2, G3 and G4, on an indoor treadmill, wearing Moticon's OpenGo insoles in their own shoes. Each athlete used his own skis, boots and poles. They were all familiar with treadmill skiing. The performance intensities varied between low, medium and high. The speeds and climbs were adjusted to fit the level (elite/intermediate) of the athletes (table 2.1). All performances were filmed by video cameras, capturing the athletes both from a front and a rear angle.

Table 2.1: Climb and speed variables

Gear	**Intensity**	**Climb [%]**	**Elite speed [km/h]**	**Intermediate speed [km/h]**
4	Low	3	13	10
4	Mid	3	16	13
4	High	3	21	16
3	Low	5	12	9
3	Mid	5	15	12
3	High	5	18	15
2	Low	12	6	5
2	Mid	12	8	6
2	High	12	10	8

In November 2016, data from recordings under snow condition was collected. One selected elite athlete performed 30 seconds intervals (of medium intensity and no climb) of the G2, G3 and G4 subtechniques. The athlete wore his own skis, poles and boots, with Moticon's OpenGo insoles.

2.1.1 Raw data

Moticon's OpenGo insoles output the following variables: 13 pressure sensors (only recording the horizontal force component), 3-axis accelerometer, total force (calculated) and CoP (calculated, illustrated in figure 2.1). The insoles had a recording frequency of 50 Hz, and they collected data separately on the right/left sole. The CoP calculation of the OpenGo system is based on the pressure sensor values and the position of their centroids in reference to the global coordinate system of the sensor insole.

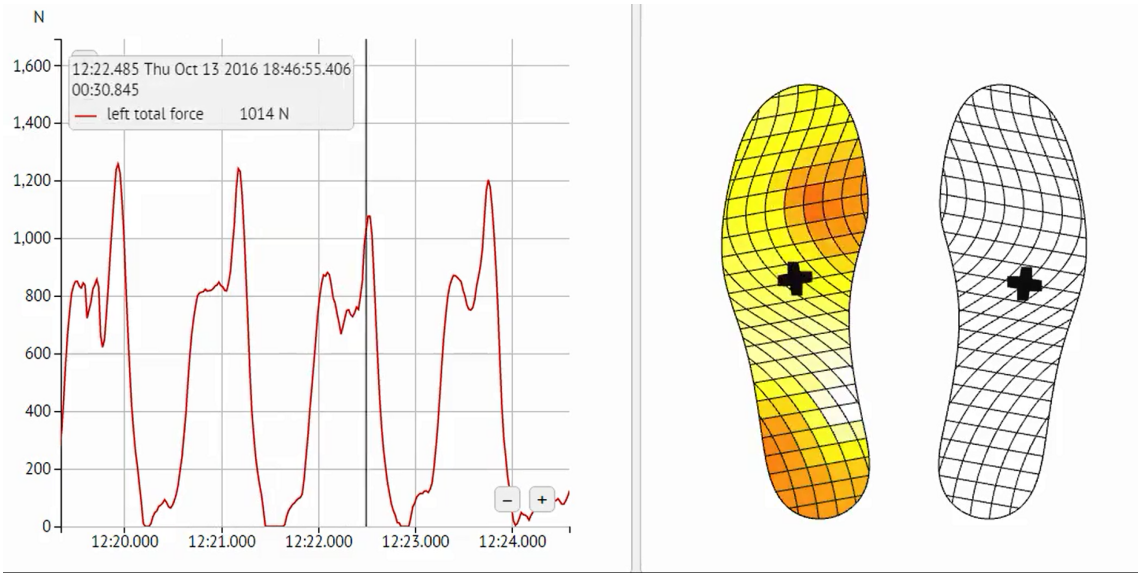

Figure 2.1: Total force (left) and CoP (right) screenshot from Moticons software

2.1.2 Data structure

The data was imported to Matlab, and was structured in a matrix with the different samples changing on each row. The variables (measures) were each given a seperate column, with the left foot variables first, then the right foot variables. Data from the right insoles of athletes 2 and 3 was missing and replaced with zeros.

2.1.3 Filtering

To minimize the high frequent noise, each athlete's data was filtered with a low-pass finite impulse response filter. The filter was implemented by Matlabs function designfilt() [MathWorks, 2016]. The pass and stop frequencies were found by spectral analysis. The accelerometer variables and the pressure sensor variables were found to suit a passband on 5 Hz, and a stopband on 10 Hz. The total force measurement was filtered with a 10 Hz passband and a 15 Hz stopband (figure 2.2 indicating the noise floor of the total force signal). In order to prevent time-delays (time shifts) because of the filtering, the function filtfilt() was used in Matlab. This function performs a zero-phase digital filtering in both the forward and reverse directions. This ensures no time-delay ([Oppenheim and Buck, 1999]), and is essential in keeping the signals in synchronization.

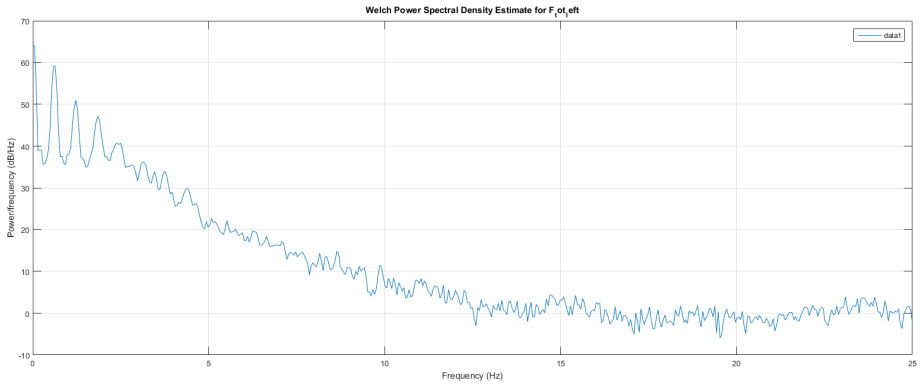

Figure 2.2: Spectral analysis of the total force measurement

2.2 Phase detection

A literature study was performed in order to find a starting point for defining different phases. The initial raw data was studied by minimizing the data to a single cycle of one foot. The cycles were determined by defining the start and end of a cycle with the trait of no force or the minimum force within a time frame (average of previous cycles) in the foot (figure 2.3). This was implemented in Matlab, and was used throughout this study.

To match the available sensor data and findings in the literature, three phases were included; gliding phase, kick phase and reposition phase. The gliding phase was defined by the period of time the ski was in contact with the ground, while not performing a kick.

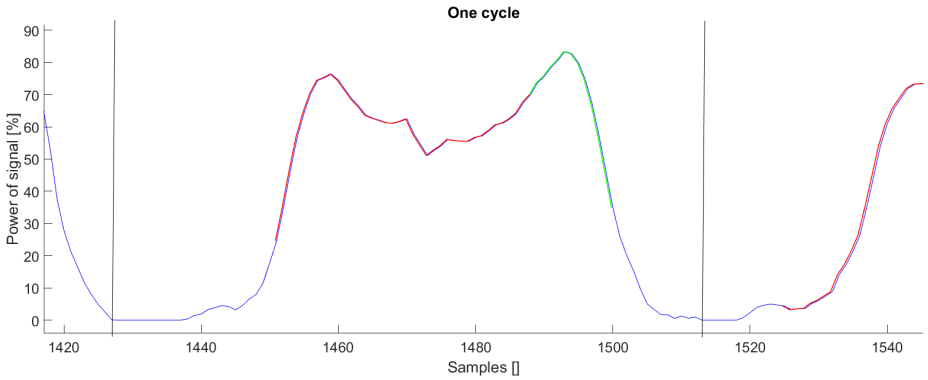

Figure 2.3: Cycle definition based on the total force in the left foot

The reposition phase was defined as the time the ski had no ground contact, and the kick phase was defined by the kick movement at the end of a gliding phase (this corresponds to Myklebust's phase definitions, without the pole plant/liftoff information [Myklebust, 2016]). It was possible to observe the phases in the total force plot (figure 2.4), which was in compliance with the literature. According to the literature, the reposition phase should have minimal to no force in the shoe. The gliding phase should start after the reposition phase when force was generated in the shoe. The kick phase was known to be around the time of maximal force in the shoe.

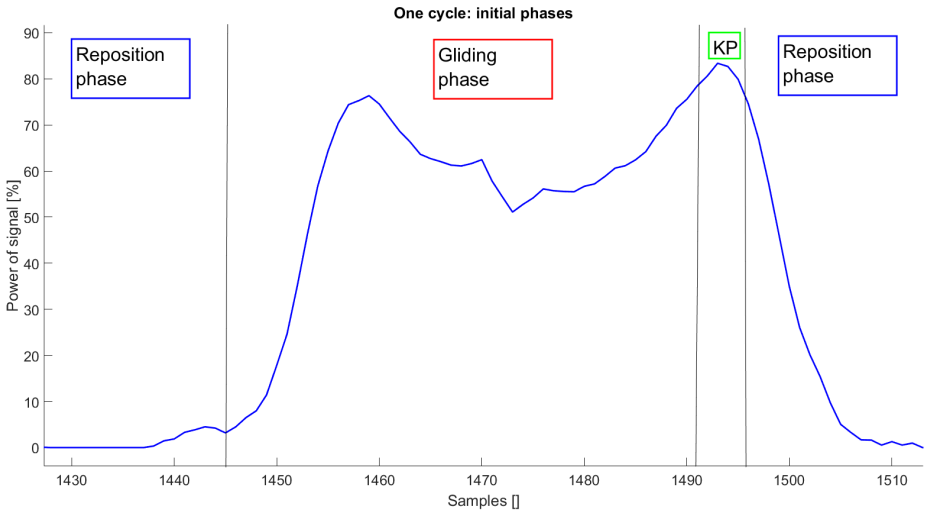

Figure 2.4: How one cycle was initially divided into different phases according to the total force graph

In order to evaluate which signals could detect differences between these phases, 10 cycles were averaged and studied in Matlab.

A biomechanical study of the changes between phases was also implemented. This

was done by analysing a 100 Hz video, including both side and back views. The changes between the reposition phase and the gliding phase, the gliding phase and the kick phase and between the kick phase and the reposition phase were analyzed. When the biomechanics and initial results were examined, features that differentiated between phases were determined. To ensure that the features were suitable for future projects, data from the insoles gathered under snow conditions were also studied. This data was however not analyzed further. With the features identified and quality assured, the algorithms were developed for one foot.

2.3 Phase time

When the phases were defined, the duration of each phase was calculated by the number of samples in each phase. The sampling rate defines the time of each sample. In this case each sample represents 0,02 seconds ([Orfanidis, 2010]).

$$F_s = \frac{1}{T} \Rightarrow T = \frac{1}{F_s} \Rightarrow T = \frac{1}{50Hz} = 0.02s \tag{2.1}$$

e.g. if a phase is 150 samples the total phase time (P) is 2 seconds.

$$P[s] = 150samples * 0.02s = 2s \tag{2.2}$$

In order to compare athletes, the average amount of time spent on each phase was calculated for each individual athlete. Cycle times and the average percentage of the cycle time the athlete spent in each phase were also evaluated and compared.

2.4 Description of the change in CoP during the gliding phase

After detecting the gliding phase, the change in CoP was visually examined. As previously stated: "When working with a data set, one of the more challenging problems is the amount of variables that need to be considered. To reduce the number of variables, one can extract features of the data set. Feature extraction is a method for construct-

ing combinations of variables that can describe the original data sufficiently [Rahmati et al., 2014]." [Garsjø, 2016]. In order to describe the change in CoP, some features were extracted based on visual results. This was done partly by the aid of statistics and partly experimentally. The features were calculated for all six athletes, and gathered in a results matrix. Each athlete's features were classified according to the level they belonged to (elite/intermediate). The complete resulting dataset was analyzed further in Unscrambler.

In order to reveal the extent of which features contributed to the dataset, a principal component analysis (PCA) was performed. "PCA can be used to extract which variables that describe the differences between samples, and which variables are correlated." [Garsjø, 2016]. Before computing the PCA, the data was normalized and the mean centered in Unscrambler. The PCA was computed by the Singular Value Decomposition algorithm [Cline and Dhillon, 2006]. One of the main results in a PCA performed with Unscrambler is the loading plot. The loading plot describes the relationship between features, and visualizes which features contribute the most to each calculated PCA. When plotting the loadings as a correlation plot, with two ellipses, the outer ellipse indicates 100% explained variance and the inner 50% explained variance. In other words, if a feature is mapped to the outer ellipse, this feature explains 100% of the PCA.

2.4.1 Cluster analysis

The new dataset with features for each athlete was oversightly enough to accommodate "visual classification". A cluster analysis was also done using Unscrambler in order to determine the potential for future classification based on these features. Cluster algorithms try to find clusters of samples that are more familiar to each other than to those in other clusters [J. Bailey, 2016]. The cluster analysis used a centroid model with a k-mean algorithm and squared Euclidean as a distance measure. The initial number of clusters were set to two (elite/intermediate). In a centroid-based cluster method, each cluster will be shown by a central object. This object can be one sample in the dataset. When performing a k-mean algorithm, it will first find K central objects, and then assign the rest into the best suited clusters (based on the distance measure). As the algorithm goes on, it tries to find better central objects to decrease the total error. The Euclidean

distance is the length of the line that connects different samples. The difference between the Euclidean distance and the squared Euclidean distance is that the squared will place grater weight on objects that are further apart [Lewicki, 2006]. The squared Euclidean distance is calculated as:

$$distance(x, y) = \sum_i (x_i - y_i)^2 \tag{2.3}$$

Chapter 3

Results

The initial results showed that there were some differences in the accelerometer data between the subtechniques. G4 was the subtechnique chosen for further investigation.

3.1 Phase detection

3.1.1 Raw data

The initial data was analyzed by solely considering the total force for one foot. The total force measurement was calculated by Moticons software, and included as a feature in the raw data. Figure 3.1 shows the total force produced by athlete 1 performing the G4 subtechnique at low intensity. The force was normalized to the average maximum signal within each cycle in order to achieve a more understandable plot. Each sample represents 0.02 seconds and the cycle time is approximately 2 seconds. The highest peaks are marked with red stars.

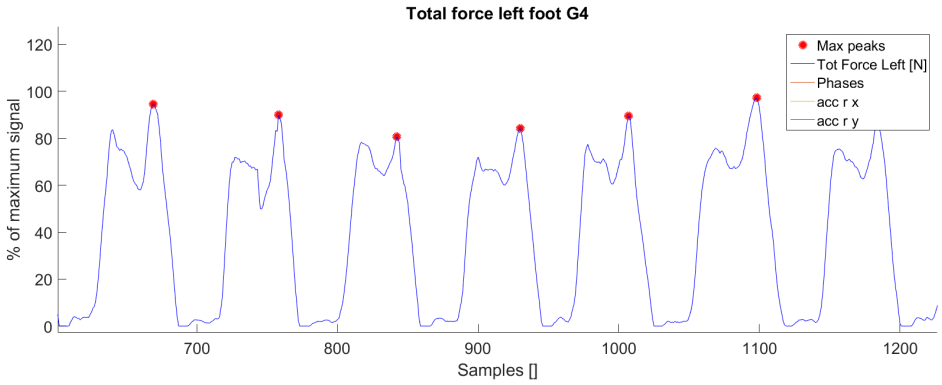

Figure 3.1: G4 low intensity performed by athlete 1, total force in left foot. Red stars mark the maximum value inside each cycle.

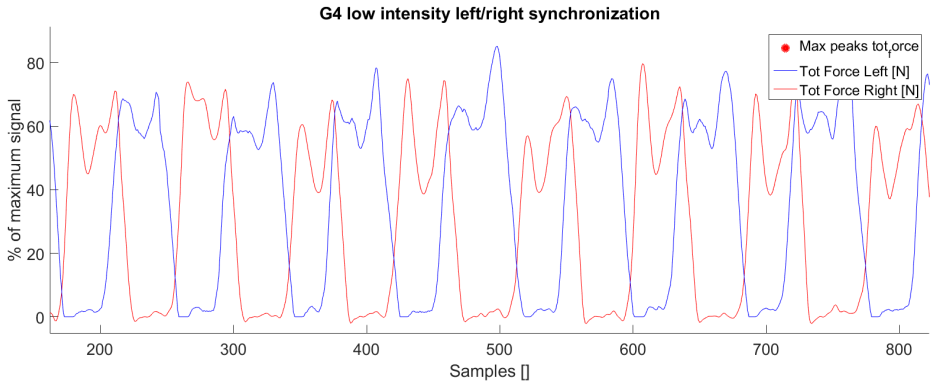

Figure 3.2: G4 low intensity performed by athlete 1, total force in left and right foot.

The right and left feet were compared so as to achieve a better understanding of the data. Figure 3.2 shows the total force produced by each leg compared to the same attributes as in the previous plot. The comparison plot (as well as other studies of the data) shows that the left and right feet perform the same movement (even though the synchronization and balance cause a different magnitude and timing). Consequently studies of one foot only was considered sufficient henceforth.

In figure 3.3 the acceleration values are plotted together with the total force. In these plots the total force curve is color coded according to the respective phases of the cycle. These plots show that some patterns occurred in every cycle, and that it was possible to detect them by extremal point detection.

Before the final "phase-change features" were chosen, the snow condition data was examined. Figure 3.4 displays the accelerometer data, as well as both feet's total force.

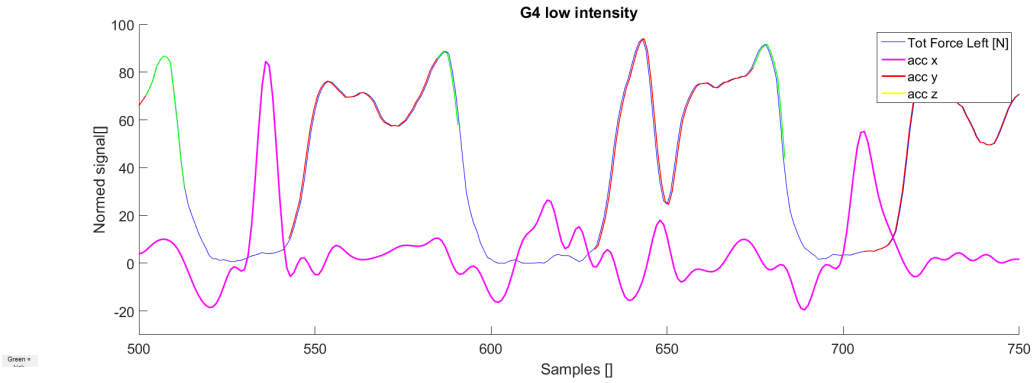

((a)) G4 low intensity acc-x data for athlete 1

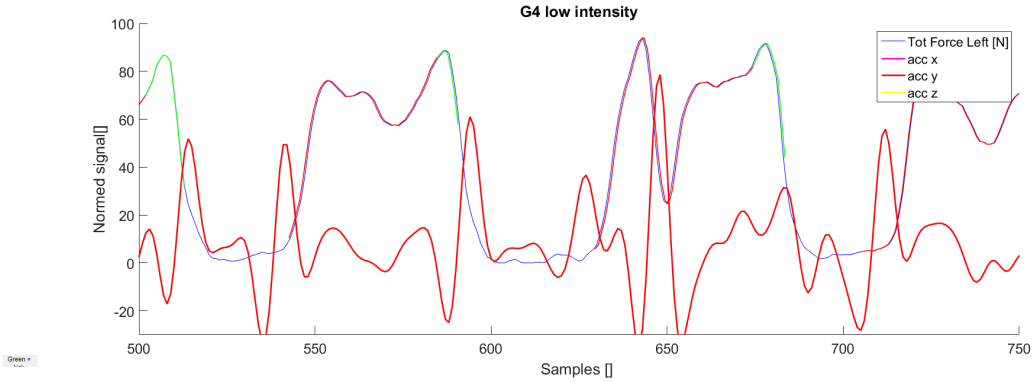

((b)) G4 low intensity acc-y data for athlete 1

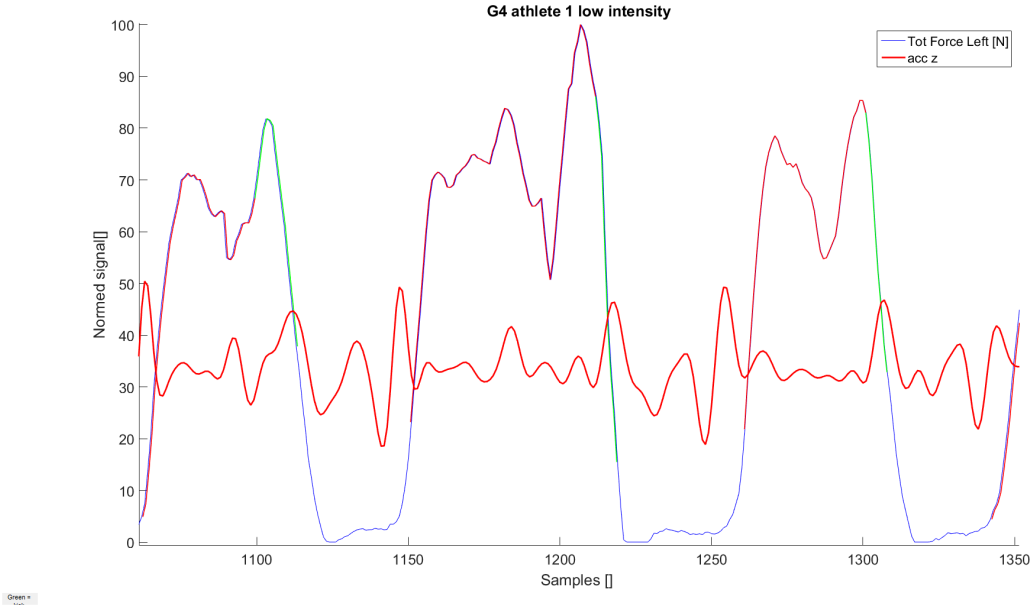

((c)) G4 low intensity acc-z data for athlete 1

Figure 3.3: Acceleration and total force plot, athlete 1, G4 low intensity. The Tot Force Left foot curve colors represent: Green = kick phase, red = gliding phase, blue = reposition phase

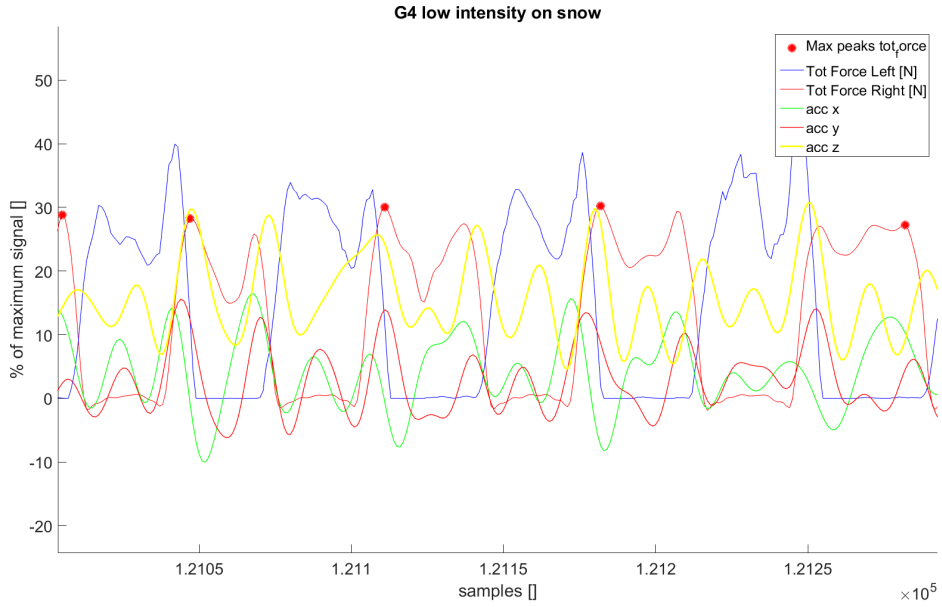

Figure 3.4: Recordings of data from snow conditions

3.1.2 Averaged data

In the search for signals describing the changes between phases, the data was averaged over 10 cycles. This worked almost as a filtering process, visualizing any repeating patterns. Figure 3.5 shows the analysis of the different subtechniques. The plots show that some signals are the same in all subtechniques, and some signals are different. The acc-x signal peaks for all subtechniques right before the total force graph rises the first time, and has the lowest recording at the end of the cycle. The acc-y signal has the same appearance, whereas the acc-z signal differs between subtechniques (even though the pattern is similar).

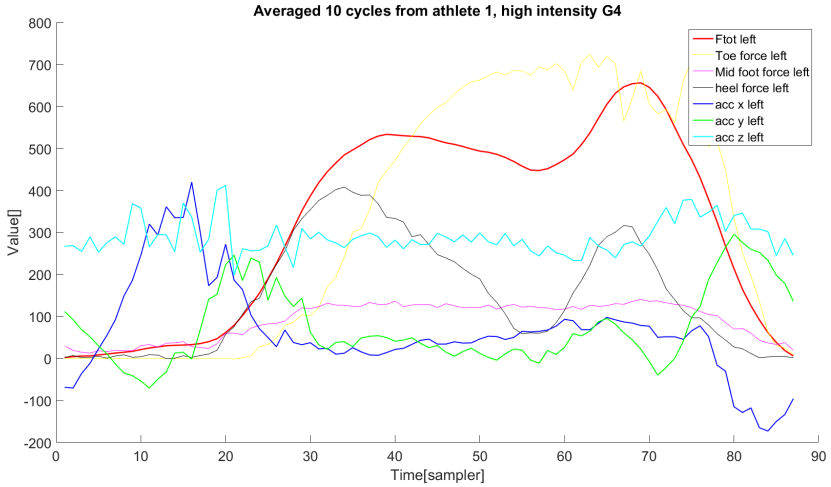

((a)) Averaged 10 cycles, plotted for athlete 1 in high G4.

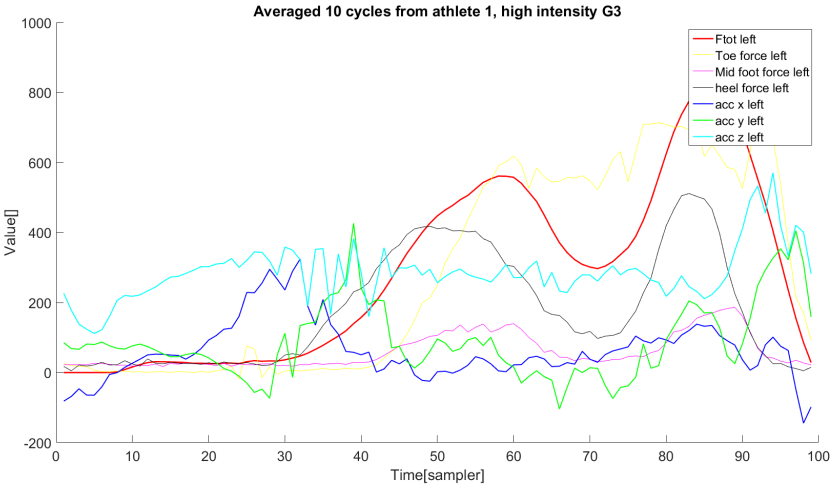

((b)) Averaged 10 cycles, plotted for athlete 1 in high G3

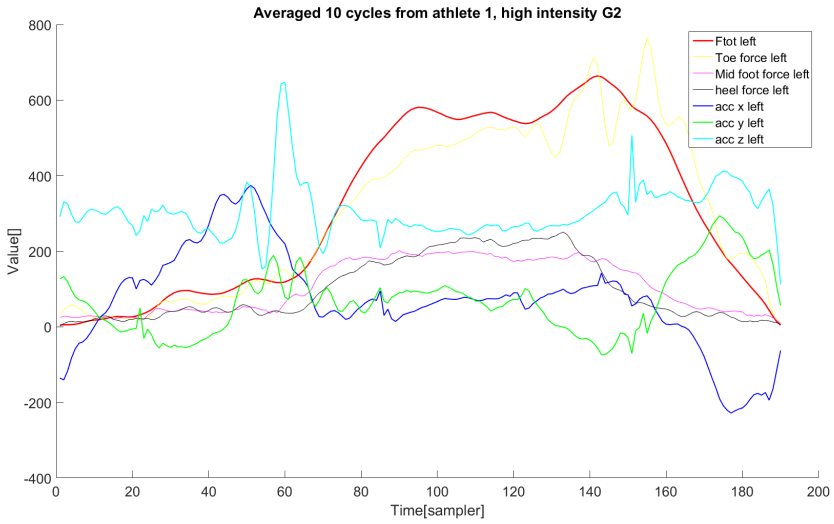

((c)) Averaged 10 cycles, plotted for athlete 1 in high G2

Figure 3.5: Averaged 10 cycles for all subtechniques.

3.1.3 Biomechanical analysis

In order to identify features characteristic of the changes between phases, a biomechanical analysis was performed. The video recorded during the data collection was used in the analysis of the skiing movements in detail, with the intention of investigating which changes could be expected in the insole data. One cycle with its according accelerometer and total force values are given in figure 3.6.

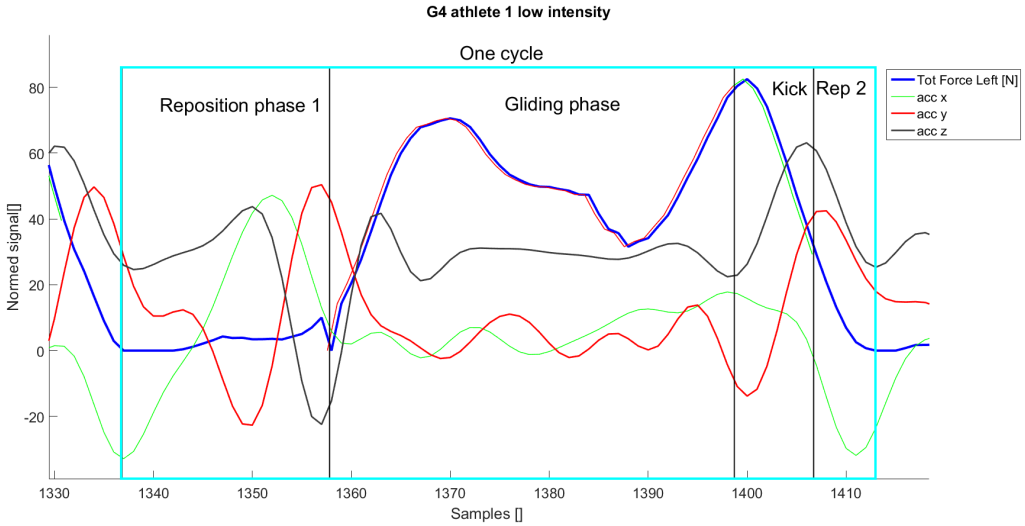

Figure 3.6: Illustration of one cycle, including the accelerometer values, reposition phase 1, gliding phase, kick phase and reposition phase 2

Start of gliding phase

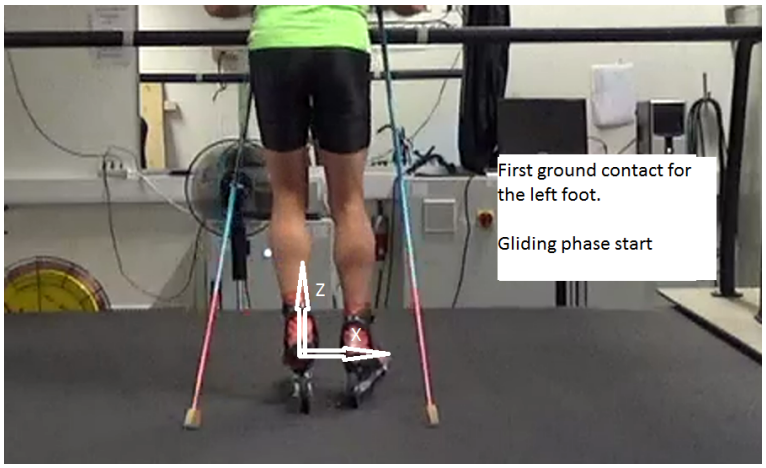

Figure 3.7: The gliding phase start in this position with the axis oriented as illustrated.

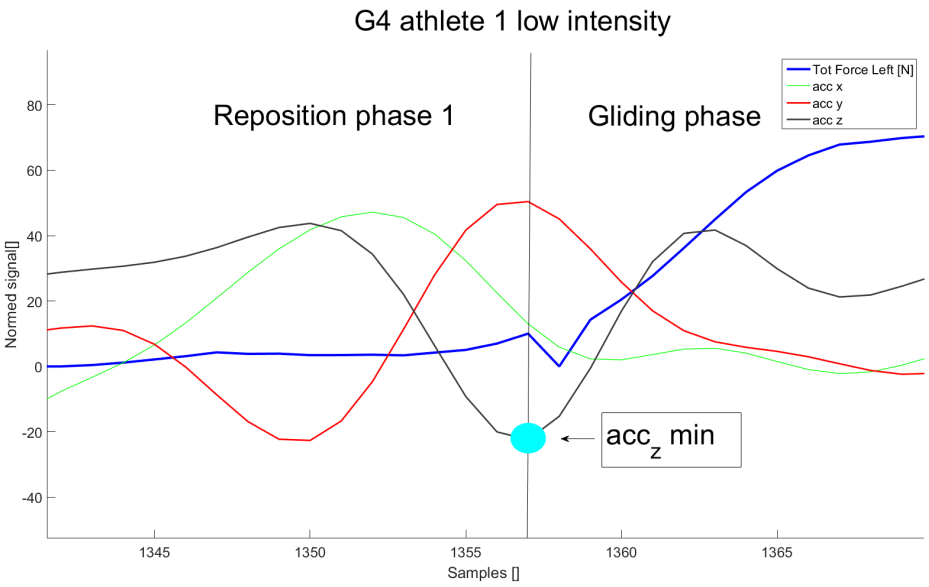

Figure 3.8: Accelerometer and insole total force data for the reposition - gliding phase change with the local minima of the acc-z value (foot plant) marked.

The gliding phase starts when the ski first makes ground contact. The foot plant is possible to detect by measuring the change in the acc-z value. This change should be a positive acceleration based on the video footage, which gives a negative value on the insole accelerometer data. Figure 3.8 shows that such point a was detected. It also shows other extremal points for the recorded acceleration. The acc-x variable has had a positive growth, changed to a negative growth and then stabilized around zero (figure 3.6). At the end of the kick phase, the athlete lifts his foot upwards before moving it along the x-axis, which results in a negative value on the acc-x variable. After this movement the leg is moved outwards again until the first ground contact is made. When acc-x passes the zero-line the leg has already started the acceleration outwards again (opposite of x-axis). According to the video, the first ground contact of the ski will take place right after the acc-x changes direction.

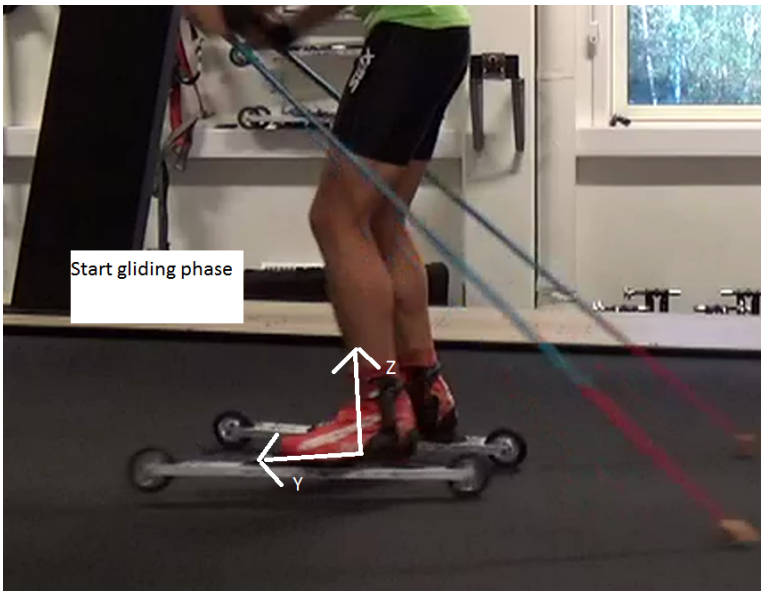

Figure 3.9: This image shows the axis orientations at the start of the gliding phase from a side angle

The acc-y variable starts at a negative value. It then passes zero and reaches a positive spike before the value starts sinking again (figure 3.8). Prior to the foot plant the athlete has moved the foot a bit along the opposite direction of the y-axis, and achieves a positive acceleration in the y-direction (negative acc-y value). This maximal value of the acc-y signal is therefore not a clear point of change, but an indicator that the change is about to happen.

Start of kick phase

((a)) Picture of athlete 1 at the start of the kick phase, with the orientation of the accelerometer axis shown from rear angle

((b)) Picture of athlete 1 at the start of the kick phase, with the orientation of the accelerometer axis shown from side angle

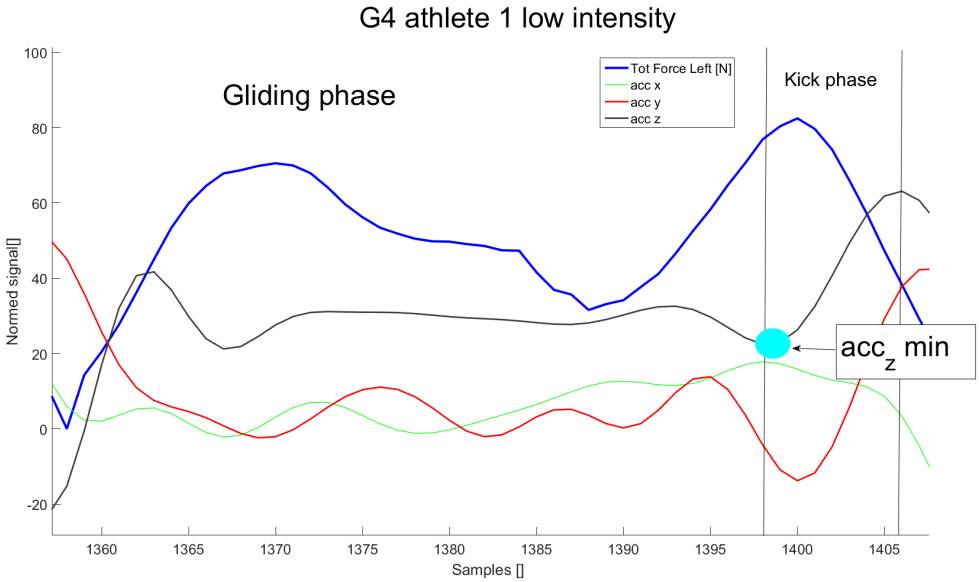

((c)) Accelerometer and insole total force data for the gliding - kick phase change with the local minima of the acc-z value marked.

Figure 3.10: Start of kick phase

In the beginning of the kick phase the athlete accelerates his foot down along the z-axis generating force. This can be observed in figure 3.10 (c) by a rapid positive change in the acc-z value. The kick phase starting point could thereby be identified by the minimal point of the acc-z value. The video shows no distinct change in movement in the x-direction.

This is consistent with the results shown in figure 3.10 (c).

In figure 3.10 (b) the start of the kick phase is shown from a side angle. When the kick movement begins, the athlete starts moving the foot along the y-axis, before a small lift of the heel. This gives a positive value in the y-direction as the foot gets "dragged" backwards. The foot is then pushed forwards (negative value) and the kick ends with a positive value when the shoe is moved in the opposite direction. Figure 3.10 (c) shows the negative growth of the y-signals just before the kick phase begins.

Start of reposition phase

The reposition phase starts when the kick ends in the position shown in figure 3.11. The kick phase is finished when the athlete changes his movement from pushing forward along the y-axis, to lifting the shoe along the negative y-axis. In figure 3.12 the acc-y value changes from a negative growth to positive one. When an athlete starts an acceleration along the z-axis he has already started to lift his foot and has moved on to the reposition phase. This is possible to detect when the acc-z reaches the maximum value. The acc-x value changes from positive to negative at the end of the kick phase. The transition from the kick phase to the reposition phase takes place when the accelerometer value crosses the zero-line. This is consistent with a logical point of view as this is the outer point of the x-axis path of motion.

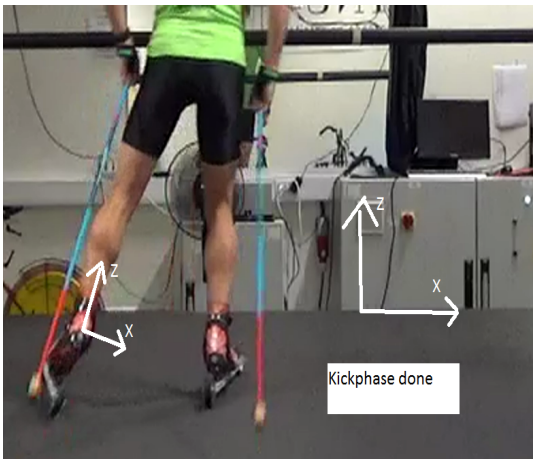

((a)) Picture of athlete 1 finishing the kick phase, with the orientation of the accelerometer axis shown from rear angle

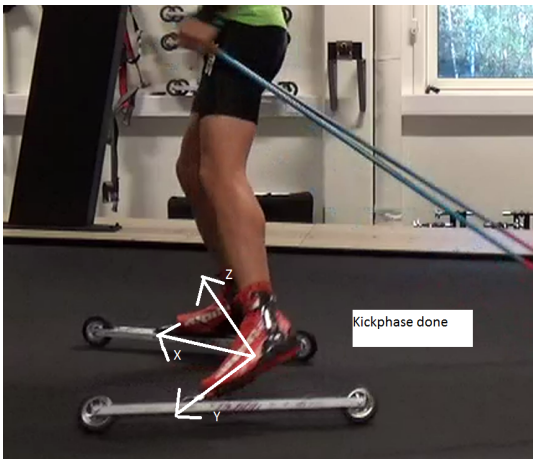

((b)) Picture of athlete 1 finishing the kick phase, with the orientation of the accelerometer axis shown from side angle

Figure 3.11: End of kick phase

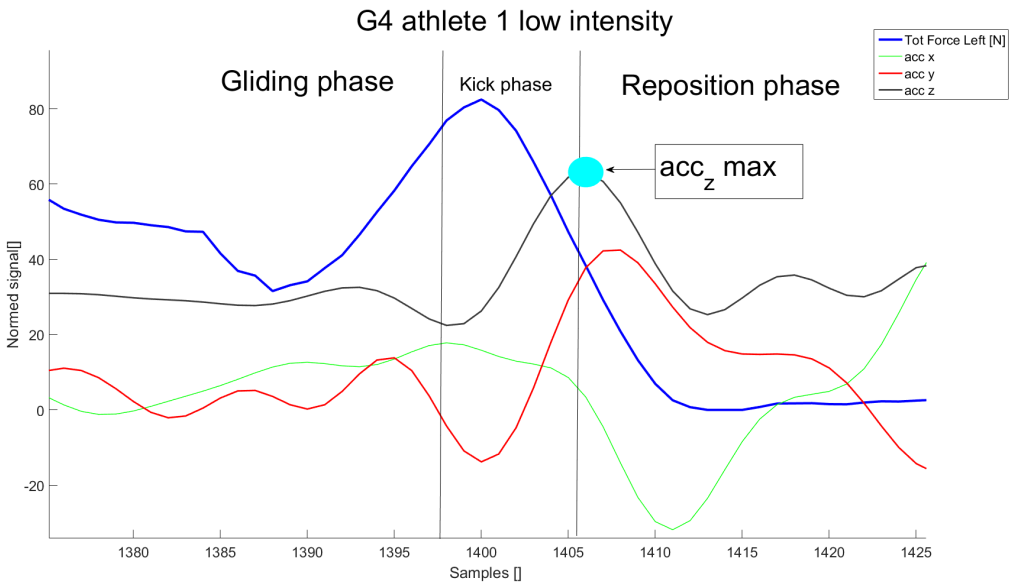

Figure 3.12: Accelerometer and insole total force data for the kick - reposition phase change with the local maxima (foot liftoff) of the acc-z value marked.

3.1.4 Phase definitions

It was desirable to identify features describing the changes between phases. The discussion regarding this will be given in section 4.1.4. Table 3.1 sums up the definitions of the beginning of each phase. These definitions are only valid within a single cycle, and are based on prior knowledge of theire order of appearance, and can not be used counterwise. For illustration purposes and for explaining the implemented algorithm, the reposition phase is divided into two phases (before and after the gliding phase).

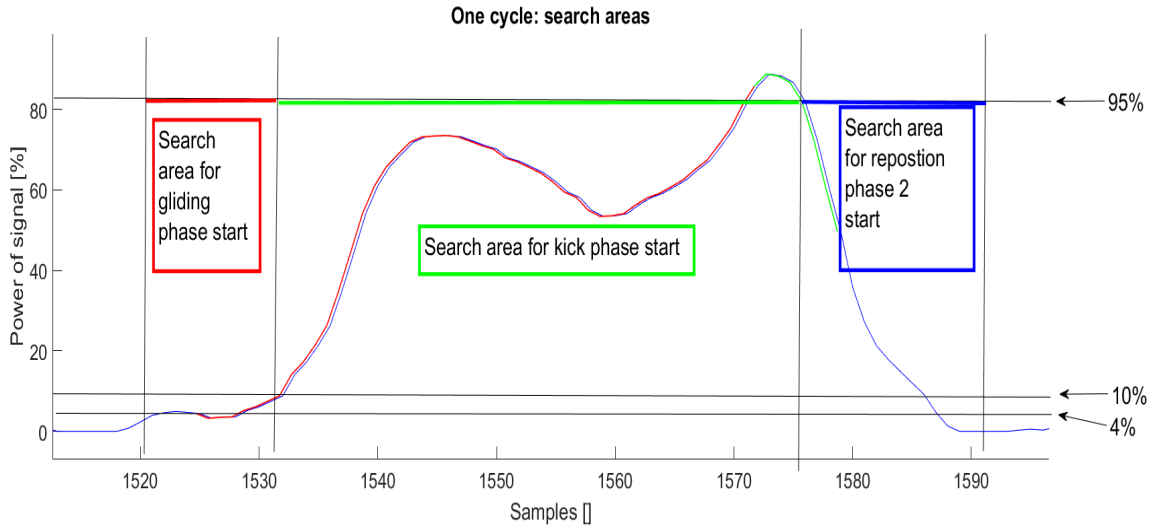

Figure 3.13: Illustration of were the search areas were defined

The total force variable was used in order to limit the search areas for the local extreme values. The total force variable was normalized to the the maximal value within each cycle, so e.g. 95% means 95% of the maximum value within that cycle. The beginning of the gliding phase search area was defined from 4% to 10%. Reposition phase 2 (following the kick phase) finished at the end of the cycle and began at 95% of total force prior to this. The beginning of the kick phase was found through a backwards search from the beginning of the reposition phase 2 to the end of the gliding phase. The search areas are illustrated in figure 3.13.

Table 3.1: Definitions of the start point of each phase

Subtechnique	**Start**
Repositioning phase 1	1) The timestamp (i) is the first within a cycle
Gliding phase	1) The last timestamp (i-1) was classified as reposition phase 2) Local minima in acc-z in given search area
Kick phase	1) The last timestamp (i-1) was classified as gliding phase 2) Local minima in acc-z in given search area
Reposition phase 2	1) The timestamp (i-1) was classified as kicking phase 2) Local maxima in acc-z in search area

3.1.5 Phase detection

The algorithm was applied on all subjects in all subtechniques. The algorithm starts by identifying the cycles, then it detects the extremal points for the acc-z value (figure 3.14 and 3.15).

Some complete phase detection results are shown in figures 3.16, 3.17 and 3.18. The results from all the athletes' G4 performances are listed in the appendix (figures 5.2 5.3, 5.4, 5.5 and 5.6)

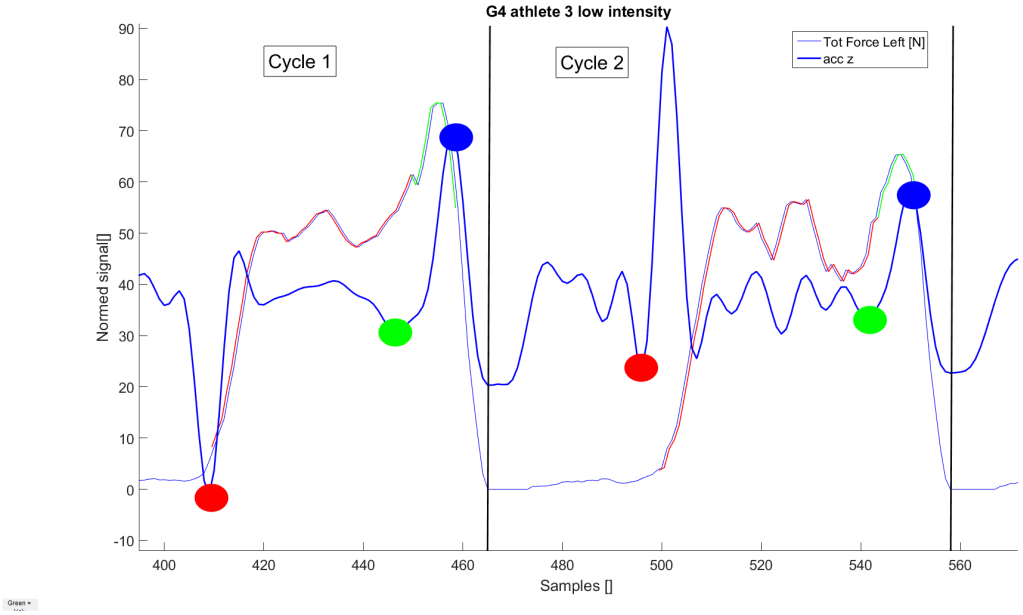

Figure 3.14: Phase detection, athlete 3, G4, high intensity. The dots represent the extremal point searched by the algorithm. The total force is colored coded according to the phases detected. Red = gliding phase, blue = reposition phase and green = kick phase.

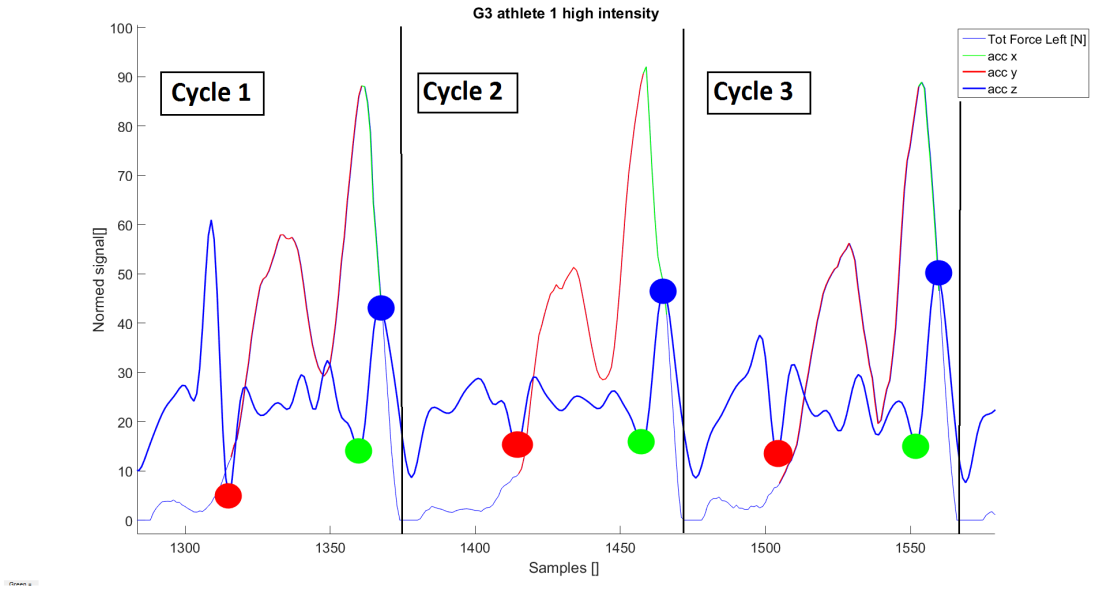

((a)) Phase detection for athlete 1 in G3 high intensity

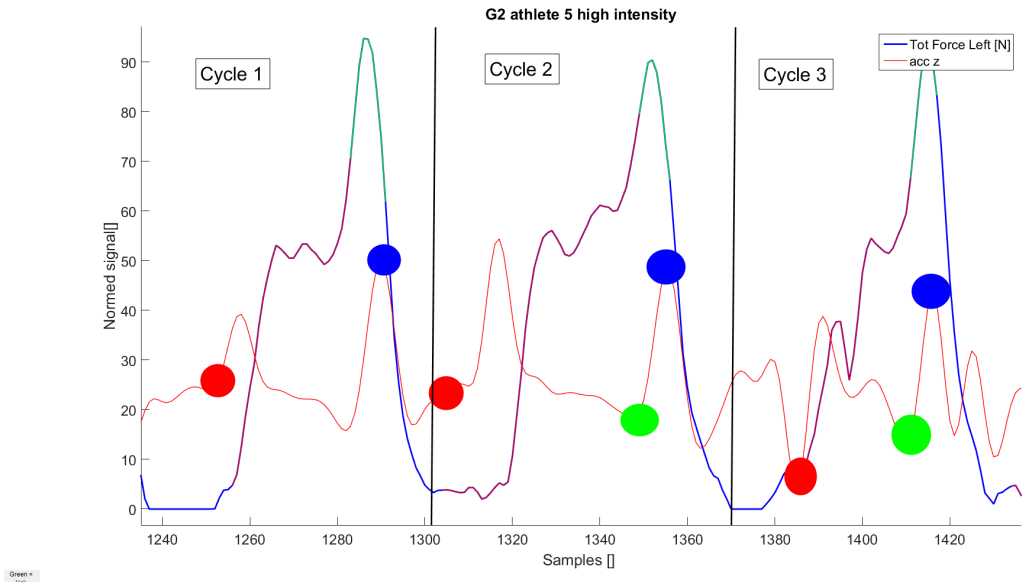

((b)) Phase detection for athlete 5 in G2 high intensity

Figure 3.15: The dots represent the extremal point searched by the algortihm. The total force is colored coded according to the phases detected. Red = gliding phase, blue = reposition phase and green = kick phase.

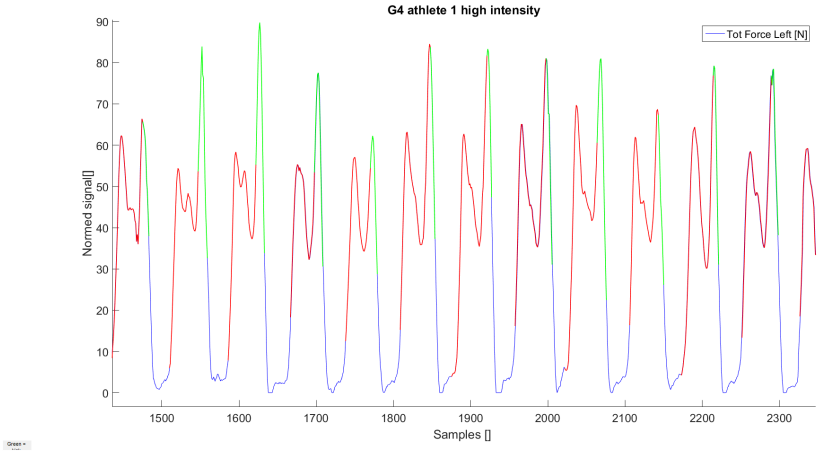

Figure 3.16: Phase detection for athlete 1 in G4 high intensity. Red = gliding phase, blue = reposition phase and green = kick phase.

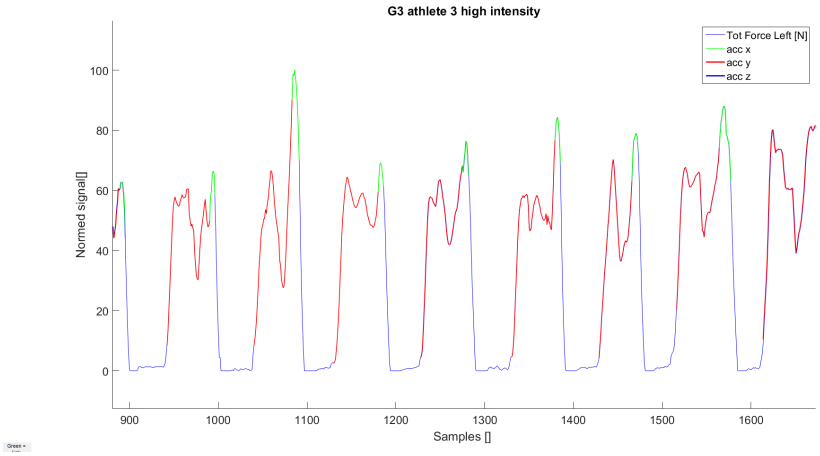

Figure 3.17: Phase detection for athlete 3 in G3 high intensity. Red = gliding phase, blue = reposition phase and green = kick phase.

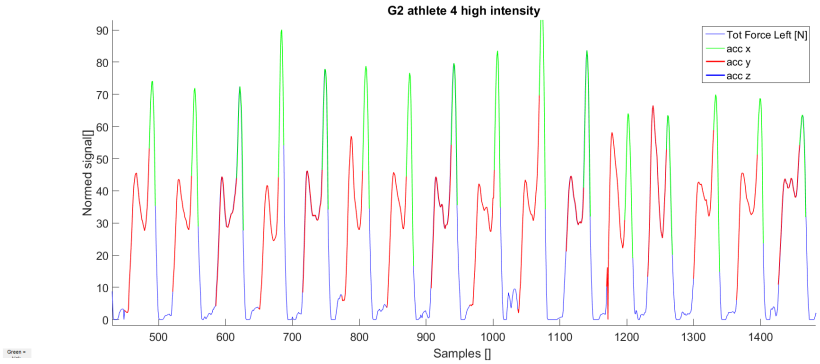

Figure 3.18: Phase detection for athlete 4 in G2 high intensity. Red = gliding phase, blue = reposition phase and green = kick phase.

3.2 Phase time

Table 3.2 lists the respective phase times for 10 cycles completed by athlete 1 performing the G4 subtechnique in high speed. The average cycle time (CT) is 1.55 seconds and the athlete spends 50% of the time on average in the gliding phase, 11% in the kick phase and 36% in the reposition phase. Table 3.3, lists the results from the same athlete performing subtechnique G2. The average CT is then 1.17 seconds, and he spends 38% of a cycle in the gliding phase, 19% in the kick phase and 36% in the reposition phase on average. There is a difference of 8% between the athlete's average kick phases in the two subtechniques.

Table 3.2: Calculated times of each phase, athlete 1, G4, high speed.

Cycle #	**Cycle time [s]**	**Gliding phase [s]**	**Kick phase [s]**	**Reposition phase[s]**
1	1,70	0,98	0,14	0,98
2	1,61	0,94	0,12	0,94
3	1,55	0,72	0,12	0,72
4	1,67	0,82	0,14	0,82
5	1,54	0,82	0,22	0,82
6	1,45	0,68	0,14	0,68
7	1,57	0,6	0,22	0,6
8	1,71	0,60	0,18	0,88
9	1,42	0,88	0,12	0,82
10	1,53	0,82	0,12	0,96

	Mean	**Std**	**Mean**	**Std**	**Mean**	**Std**	**Mean**	**Std**
Average time [s]	1.55	0,28	0,78	0.13	0.16	0.05	0.46	0,17
Average % of a cycle			0,50		0,11		0,36	

Table 3.3: Calculated times of each phase, athlete 1, G2, high speed.

Cycle #	**Cycle time** [s]	**Gliding phase** [s]	**Kick phase** [s]	**Reposition phase**[s]
1	1.30	0.50	0.28	0.52
2	1.31	0.42	0.20	0.69
3	1.29	0.56	0.22	0.51
4	1.35	0.38	0.32	0.65
5	1.39	0.72	0.30	0.37
6	1.18	0.48	0.14	0.56
7	1.35	0.64	0.26	0.45
8	1.19	0.54	0.26	0.39
9	1.34	0.48	0.20	0.66
10	1.25	0.46	0.30	0.49

	Mean	**Std**	**Mean**	**Std**	**Mean**	**Std**	**Mean**	**Std**
Average time [s]	1.17	0,25	0,46	0.13	0.23	0.07	0.46	0,14
Average % of a cycle			0,38		0,19		0,36	

The complete set of calculated phase times for each athlete performing the subtechnique G4, is listed in the appendix (table 5.1, 5.2, 5.3, 5.4, 5.5, 5.6). The average results for the G2 and G4 subtechniques are presented in table 3.4, 3.5, 3.6 and 3.7.

Table 3.4: Average statistics for all athletes performing the G4 subtechnique

	Cycle time [s]		**Gliding phase** [s]		**Kick phase** [s]		**Reposition phase**[s]	
	Mean	Std	Mean	Std	Mean	Std	Mean	Std
Average time [s]	1.58	0.10	0.79	0.13	0.15	0.01	0.56	0.11
% of a cycle			0.50	0.07	0.09	0.01	0.35	0.06

Table 3.5: Average statistics for all athletes performing the G2 subtechnique

	Cycle time [s]		**Gliding phase** [s]		**Kick phase** [s]		**Reposition phase**[s]	
	Mean	Std	Mean	Std	Mean	Std	Mean	Std
Average time [s]	1.35	0.44	0.65	0.34	0.18	0.07	0.52	0.20
% of a cycle			0.46	0.09	0.12	0.04	0.36	0.08

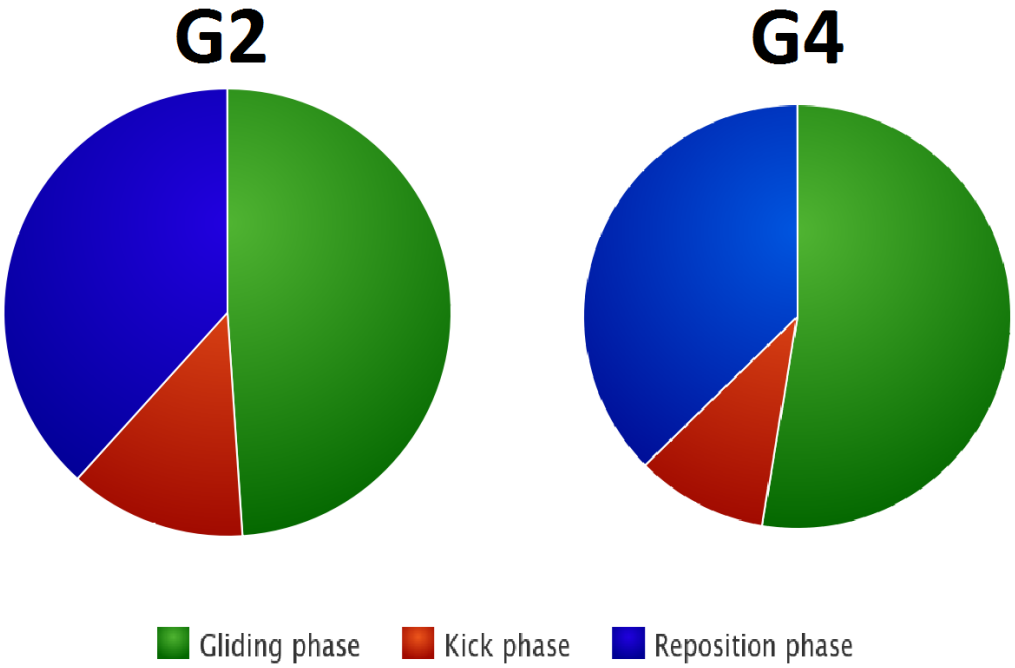

Figure 3.19: Average time spent in each phase for all athletes performing the G4 and G2 subtechnique within high intensity.

Table 3.6: Average phase time for each athlete performing the G4 subtechnique

	Cycle time [s]		**Gliding phase [s]**		**Kick phase [s]**		**Reposition phase[s]**	
	Mean	Std	Mean	Std	Mean	Std	Mean	Std
Intermediate level								
Athlete 2	1.87	0.51	0.80	0.24	0.18	0.06	0.74	0.23
Athlete 3	1.62	0.41	0.77	0.23	0.13	0.04	0.71	0.20
Athlete 4	1.52	0.38	0.64	0.17	0.18	0.05	0.69	0.19
Min	1.52	0.38	0.64	0.17	0.13	0.04	0.69	0.19
Max	1.87	0.51	0.80	0.24	0.18	0.06	0.74	0.23
Average	1.67	0.43	0.73	0.21	0.16	0.05	0.71	0.20
Elite level								
Athlete 1	1.50	0.28	0.78	0.13	0.17	0.05	0.55	0.13
Athlete 5	1.46	0.37	0.82	0.29	0.14	0.05	0.49	0.17
Athlete 6	1.53	0.37	0.92	0.35	0.14	0.03	0.46	0.26
Min	1.46	0.28	0.78	0.13	0.14	0.03	0.46	0.13
Max	1.53	0.37	0.92	0.35	0.17	0.05	0.55	0.26
Average	1.49	0.34	0.84	0.25	0.15	0.04	0.50	0.18

Table 3.7: Average phase time for each athlete performing the G2 subtechnique

	Cycle time [s]		**Gliding phase [s]**		**Kick phase [s]**		**Reposition phase[s]**	
	Mean	Std	Mean	Std	Mean	Std	Mean	Std
Intermediate level								
Athlete 2	1.87	0.51	0.80	0.24	0.18	0.06	0.74	0.23
Athlete 3	1.33	0.28	0.51	0.12	0.14	0.04	0.62	0.16
Athlete 4	1.36	0.33	0.66	0.22	0.18	0.05	0.46	0.15
Min	1.33	0.28	0.51	0.12	0.14	0.04	0.46	0.15
Max	1.87	0.51	0.80	0.24	0.18	0.06	0.74	0.23
Average	1.52	0.37	0.66	0.19	0.17	0.05	0.61	0.18
Elite level								
Athlete 1	1.17	0.25	0.46	0.13	0.23	0.07	0.46	0.14
Athlete 5	1.33	0.34	0.64	0.27	0.16	0.04	0.46	0.16
Athlete 6	1.87	0.79	1.14	0.68	0.15	0.05	0.41	0.18
Min	1.17	0.25	0.46	0.13	0.15	0.04	0.41	0.14
Max	1.87	0.79	1.14	0.68	0.23	0.07	0.46	0.18
Average	1.46	0.46	0.75	0.36	0.18	0.05	0.44	0.16

Figure 3.20 shows the calculated times. In each plot, the elite and intermediate athletes are grouped. In the elite group they are plotted in the order: 1, 5 and 6. In the intermediate group the athletes are plotted in the order: 2, 3, 4. The elite athletes had longer gliding phases than did the intermediate athletes both in the performance of the G4 and the G2 subtechniques. The reposition time was a bit longer for the intermediate group than the elite athletes during the performance of both subtechniques.

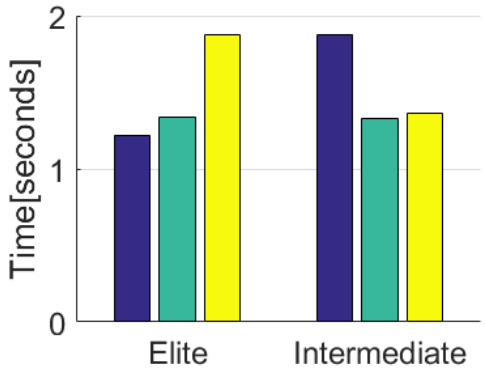

((a)) CT for each athlete in G2 high intensity

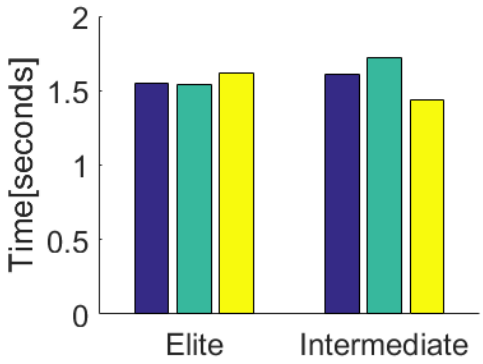

((b)) CT for each athlete in G4 high intensity

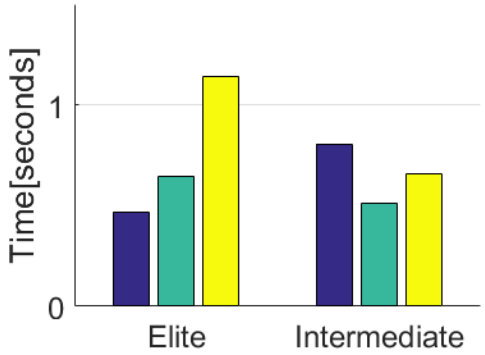

((c)) Gliding time for each athlete in G2 high intensity

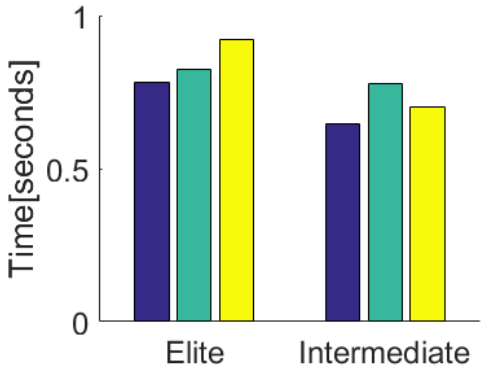

((d)) Gliding time for each athlete in G4 high intensity

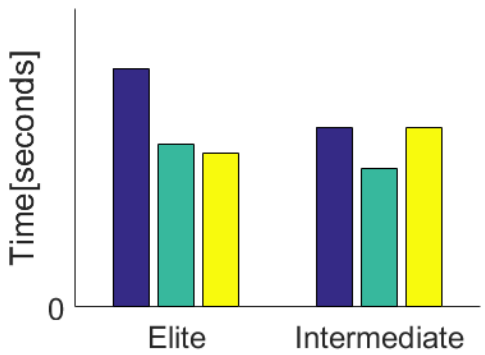

((e)) Kick time for each athlete in G2 high intensity

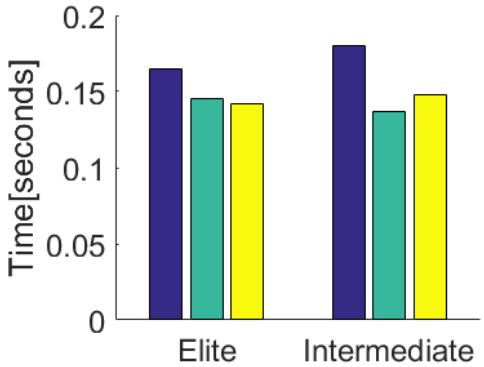

((f)) Kick time for each athlete in G4 high intensity

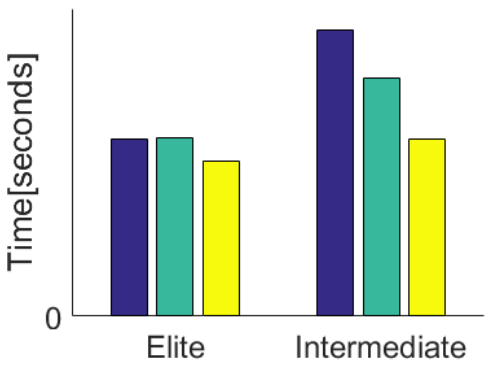

((g)) Reposition time for each athlete in G2 high intensity

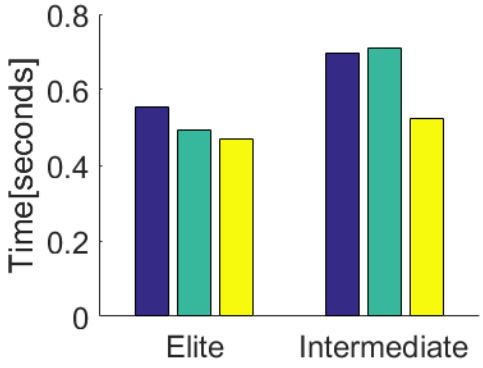

((h)) Reposition time for each athlete in G4 high intensity

Figure 3.20: Average phase time for elite [Athlete: 1,5,6] and intermediate [Athlete: 2,3,4]

3.3 Change in CoP during the gliding phase

All athletes had a common pattern in the change of CoP during the gliding phase when performing the G4 subtechnique (figure 3.21). The athletes start the phase with the CoP in the center of the foot lateral-/medialwise (x-direction). The center of pressure is located behind the center of the anterior/posterior center line (y-direction). The movement begins by shifting the weight forward and towards the medial side of the foot. There are differences between the athletes regarding the duration of each movement.

The change in CoP during the gliding phase in subtechnique G2 is shown in figure 3.22 for all athletes. The same pattern as described for the G4 subtechnique can be seen, but it is less distinct.

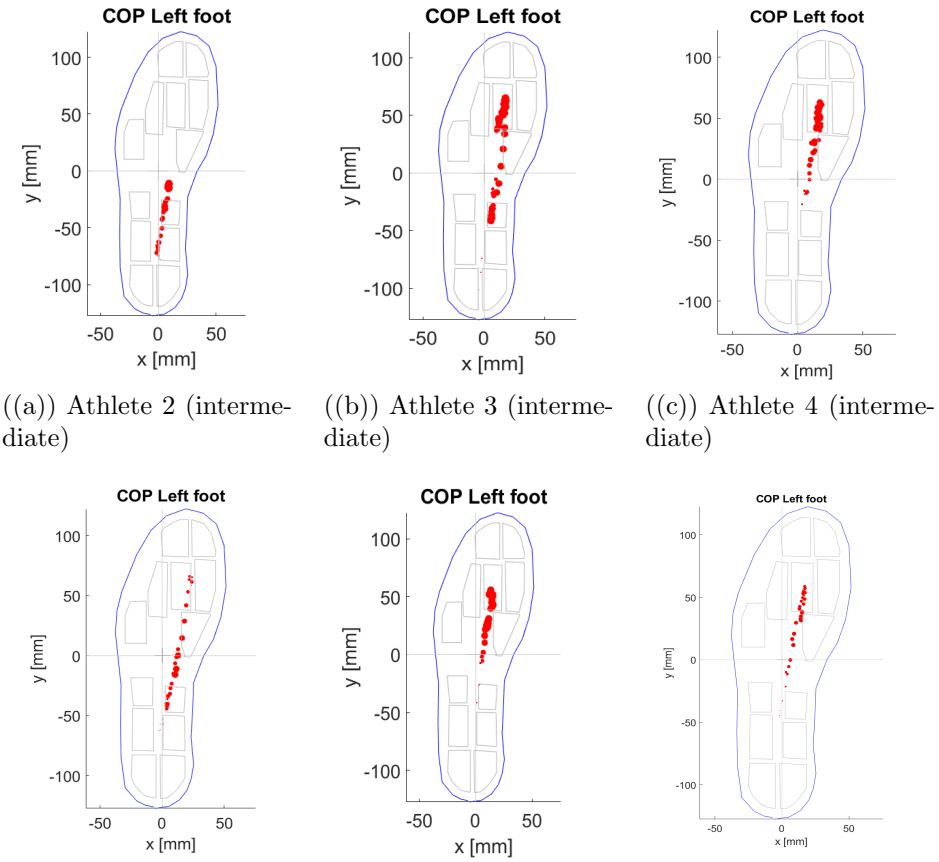

((a)) Athlete 2 (intermediate) ((b)) Athlete 3 (intermediate) ((c)) Athlete 4 (intermediate)

((d)) Athlete 1 (elite) ((e)) Athlete 5 (elite) ((f)) Athlete 6 (elite)

Figure 3.21: Change in CoP during the gliding phase, performing the G4 subtechnique, high intensity

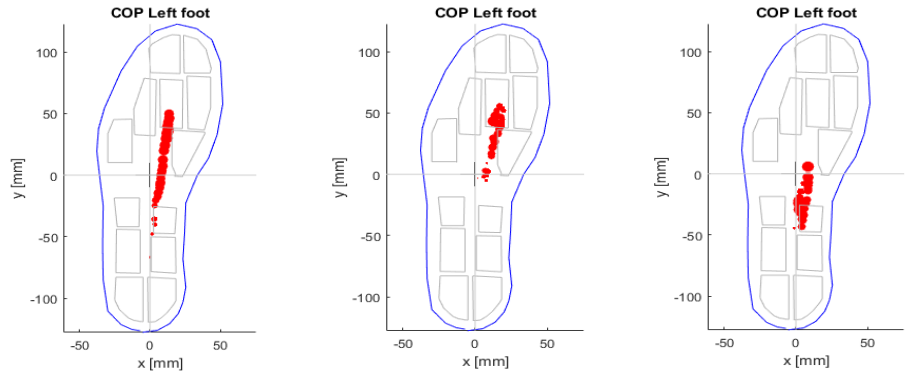

((a)) Athlete 2 (intermediate)

((b)) Athlete 3 (intermediate)

((c)) Athlete 4 (intermediate)

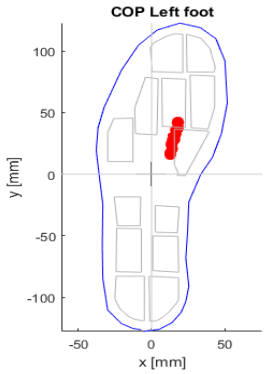

((d)) Athlete 1 (elite)

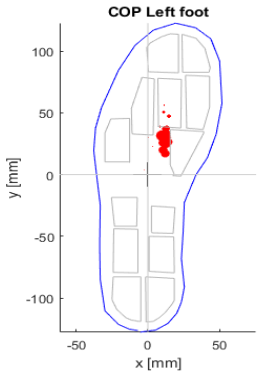

((e)) Athlete 5 (elite)

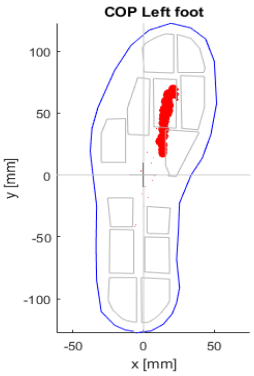

((f)) Athlete 6 (elite)

Figure 3.22: Change in CoP during the gliding phase, performing the G2 subtechnique, high intensity

3.4 Change in CoP during the kick phase

The CoP continues to move forward and towards the medial side of the foot as presented in figures 3.23 and 3.24. The change in CoP during the kick phase has a smaller magnitude than that of the gliding phase, but it includes the final change before the foot's liftoff which shifts the CoP a lot.

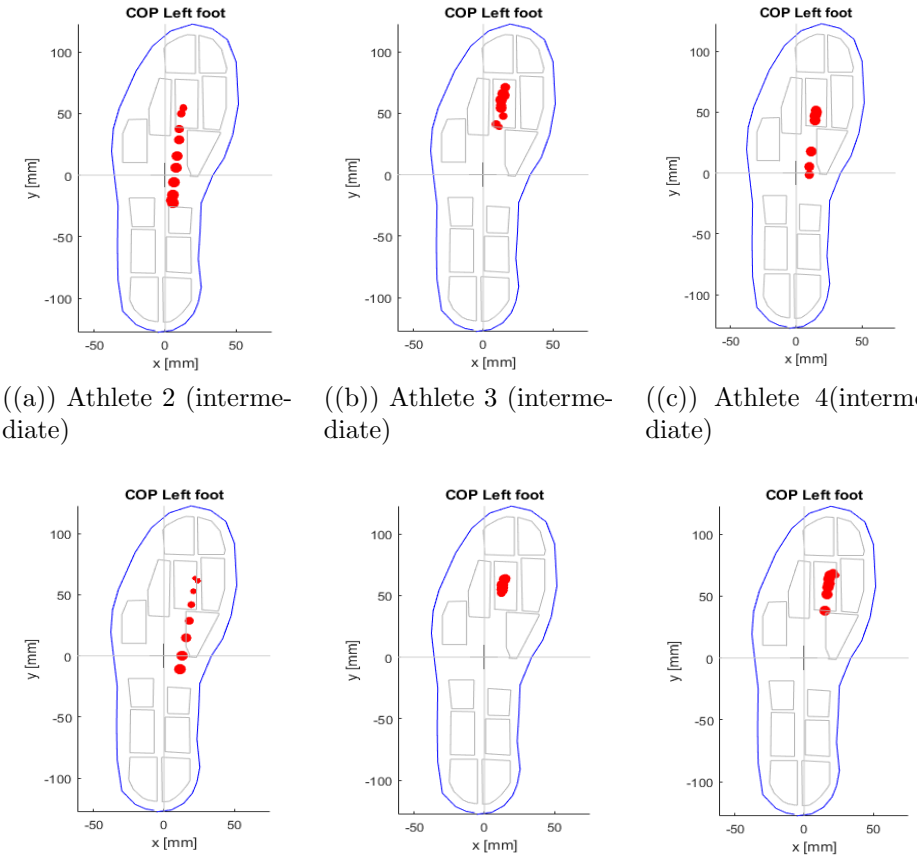

((a)) Athlete 2 (intermediate) ((b)) Athlete 3 (intermediate) ((c)) Athlete 4(intermediate)

((d)) Athlete 1(elite) ((e)) Athlete 5(elite) ((f)) Athlete 6(elite)

Figure 3.23: Change in CoP during the kick phase, performing the G4 subtechnique, high intensity

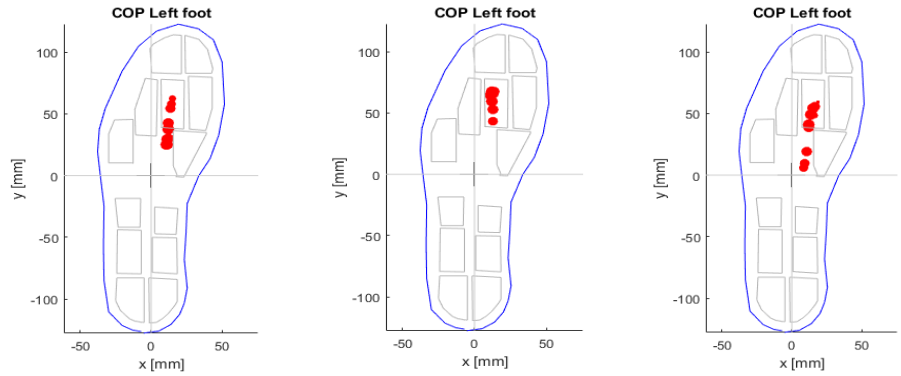

((a)) Athlete 2 (intermediate)

((b)) Athlete 3 (intermediate)

((c)) Athlete 4 (intermediate)

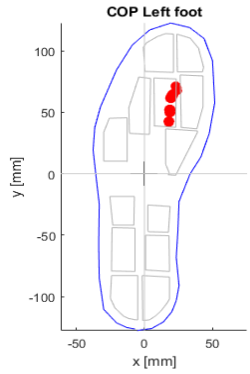

((d)) Athlete 1 (elite)

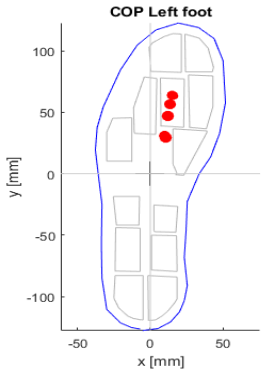

((e)) Athlete 5 (elite)

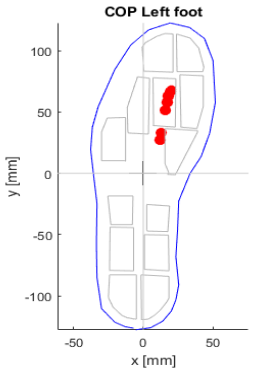

((f)) Athlete 6 (elite)

Figure 3.24: Change in CoP during the kick phase, performing the G2 subtechnique, high intensity

3.4.1 Features

The following features were included:

Delta x [mm]: The difference between the end and start position in x-direction

Delta y [mm]: The difference between the end and start position in y-direction

Theta [deg]: Polar representation of (delta x,delta y)

Rho [mm]: Polar representation of (delta x,delta y)

Start x [mm]: Where the athlete starts the gliding phase (x-pos)

Start y [mm]: Where the athlete starts the gliding phase (y-pos)

End x [mm]: Where the athlete ends the gliding phase (x-pos)

End y [mm]: Where the athlete ends the gliding phase (y-pos)

V_delta CoP X [m/s]: The speed of which the CoP changes along the gliding phase in the X-direction

V_delta CoP Y [m/s]: The speed of which the CoP changes along the gliding phase in the Y-direction

The features for the gliding phase in the G4 subtechnique performed with high intensity are shown in table 3.8 and table 3.9. The features for the gliding phase in the G2 subtechnique performed with high intensity are shown in table 3.10 and table 3.11. A comparison of the features between the elite and intermediate groups is made in figure 3.25.

Table 3.8: Calculated features for the elite athletes gliding phase, G4, high intensity

Athlete	**1**	**5**	**6**	**Average**	**Max**	**Min**
Delta x[mm]	24.62	19.16	26.51	**23.43**	**26.51**	**19.16**
Delta y[mm]	121.64	102.10	122.88	**115.54**	**122.88**	**102.10**
Theta[deg]	76.38	75.44	74.20	**75.34**	**76.38**	**74.20**
Rho[mm]	123.98	103.77	125.49	**117.75**	**125.49**	**103.77**
Start[x]	0.5631	2.31	1.51	**1.46**	**2.31**	**0.56**
Start y[mm]	-60.52	-28.82	-23.99	**-37.78**	**-23.99**	**-60.52**
End x[mm]	12.8231	10.86	13.76	**12.48**	**13.76**	**10.86**
End y[mm]	0.88	32.3974	40.90	**24.73**	**40.90**	**0.88**
V_delta CoP X[m/s]	0.03	0.02	0.02	**0.02**	**0.03**	**0.02**
V_delta CoP Y[m/s]	0.15	0.11	0.13	**0.13**	**0.1**	**0.1**

Table 3.9: Calculated features for the intermediate athletes, gliding phase, G4, high intensity

Athlete	**2**	**3**	**4**	**Average**	**Max**	**Min**
Delta x[mm]	10.60	20.54	22.77	**17.97**	**22.77**	**10.60**
Delta y[mm]	67.28	125.30	93.53	**95.37**	**125.30**	**67.28**
Theta[deg]	76.73	76.62	73.60	**75.65**	**76.73**	**73.60**
Rho[mm]	68.06	126.82	96.27	**97.05**	**126.82**	**68.06**
Start[x]	1.65	-1.55	1.51	**0.53**	**1.65**	**-1.55**
Start y[mm]	-52.25	-67.70	-38.88	**-52.94**	**-38.88**	**-67.70**
End x[mm]	8.56	12.40	10.53	**10.50**	**12.40**	**8.56**
End y[mm]	-3.05	27.87	12.37	**12.39**	**27.87**	**-3.05**
V_delta CoP X[m/s]	0.01	0.02	0.02	**0.02**	**0.02**	**0.01**
V_delta CoP Y[m/s]	0.09	0.15	0.13	**0.12**	**0.1**	**0.09**

Table 3.10: Calculated features for the elite athletes, gliding phase, G2, high intensity

Athlete	**1**	**5**	**6**	**Average**	**Max**	**Min**
Delta x[mm]	10.89	18.58	25.54	**18.34**	**25.54**	**10.89**
Delta y[mm]	40.34	53.07	78.60	**57.34**	**78.60**	**40.34**
Theta[deg]	71.56	67.83	66.60	**68.66**	**71.56**	**66.60**
Rho[mm]	41.91	56.64	82.41	**60.32**	**82.41**	**41.91**
Start x [mm]	10.24	7.22	8.08	**8.51**	**7.22**	**10.24**
Start y [mm]	31.53	34.29	17.20	**27.67**	**34.29**	**17.20**
End x [mm]	13.08	9.35	13.00	**11.81**	**13.08**	**9.35**
End y [mm]	21.88	30.37	30.41	**27.55**	**30.41**	**21.88**
V delta CoP X[m/s]	0.02	0.02	0.02	**0.02**	**0.02**	**0.02**
V delta CoP Y[m/s]	0.08	0.07	0.07	**0.07**	**0.08**	**0.07**

Table 3.11: Calculated features for the intermediate athletes, gliding phase, G2, high intensity

Athlete	**2**	**3**	**4**	**Average**	**Max**	**Min**
Delta x[mm]	12.86	10.93	13.72	**12.50**	**13.72**	**10.93**
Delta y[mm]	77.48	61.87	73.88	**71.07**	**77.48**	**61.87**
Theta[deg]	74.86	76.06	76.18	**75.70**	**74.86**	**76.06**
Rho[mm]	78.41	62.88	75.10	**72.13**	**78.41**	**62.88**
Start x [mm]	-0.30	6.72	1.31	**2.57**	**6.72**	**-0.30**
Start y [mm]	-53.34	18.44	-36.07	**-23.65**	**18.44**	**-53.34**
End x [mm]	6.65	11.13	7.65	**8.48**	**11.13**	**6.65**
End y [mm]	-2.27	24.96	7.88	**10.19**	**24.96**	**-2.27**
V delta CoP X[m/s]	0.01	0.01	0.01	**0.02**	**0.01**	**0.01**
V delta CoP Y[m/s]	0.08	0.11	0.10	**0.10**	**0.11**	**0.08**

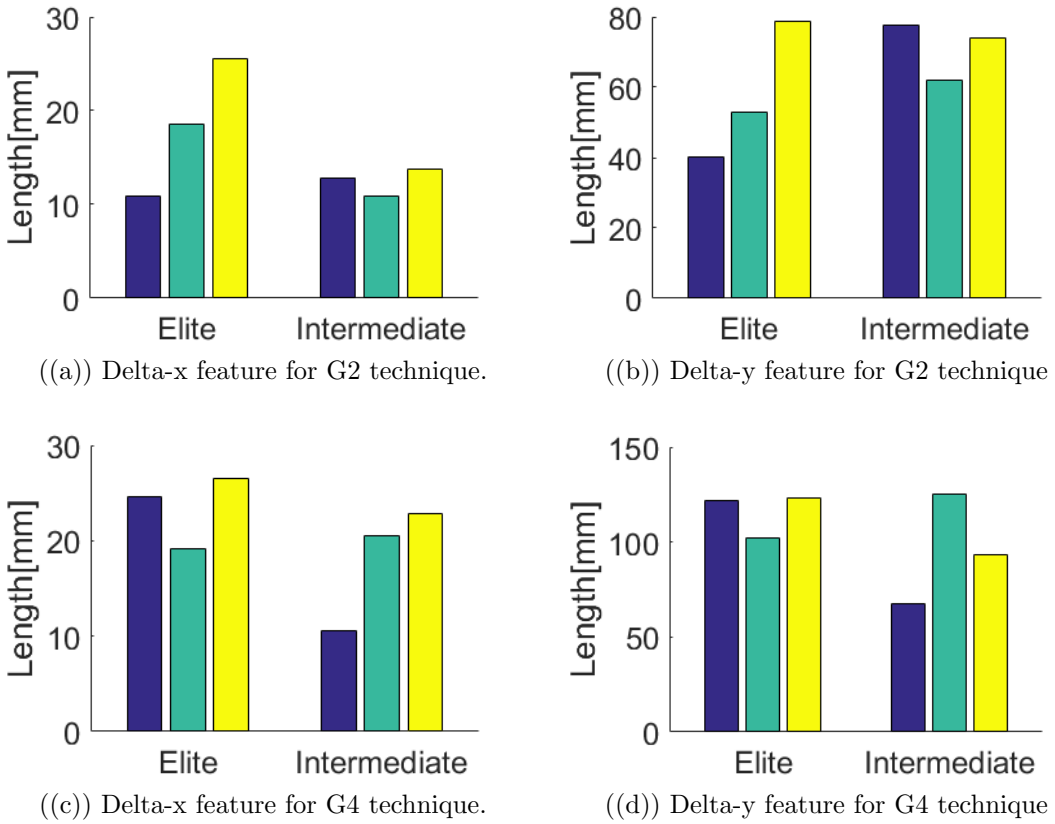

((a)) Delta-x feature for G2 technique.

((b)) Delta-y feature for G2 technique

((c)) Delta-x feature for G4 technique.

((d)) Delta-y feature for G4 technique

Figure 3.25: Comparison of delta-x and delta-y features between the elite [Athlete: 1,5,6] and intermediate [Athlete: 2,3,4] groups performing the G2 and G4 subtecnique with high intensity.

The results of the clustering calculation are shown in table 3.12. The complete overview can be found in the appendix in tables 5.12 (G4) and 5.13 (G2). This table shows that five out of six athletes were correctly classified for both the G2 and G4 sub-

techniques. Elite skiers were given the correct cluster, but one intermediate skier (athlete 3) was incorrectly given the elite cluster as well (both for G2 and G4).

Table 3.12: Cluster result for G2 and G4 subtechnique

Athlete	**Class**
1	0
2	1
3	0
4	1
5	0
6	0

3.4.2 Feature comparison

A PCA was computed in order to analyze which features best explained the data. In figure 3.26 and in table 3.13 the main PCA results for the G4 subtechnique are presented. 86% of the data were explained by two principal components. PC-1 was explained by over 97% both by delta_y and Rho. As the features represent almost the same measure, this was to be expected. The end_x feature is also highly correlated to PC-1. PC-2 is almost entirely explained by the start_y feature. This indicates that the most important features in explaining the given dataset are: delta_y/Rho, end_x and start_y.

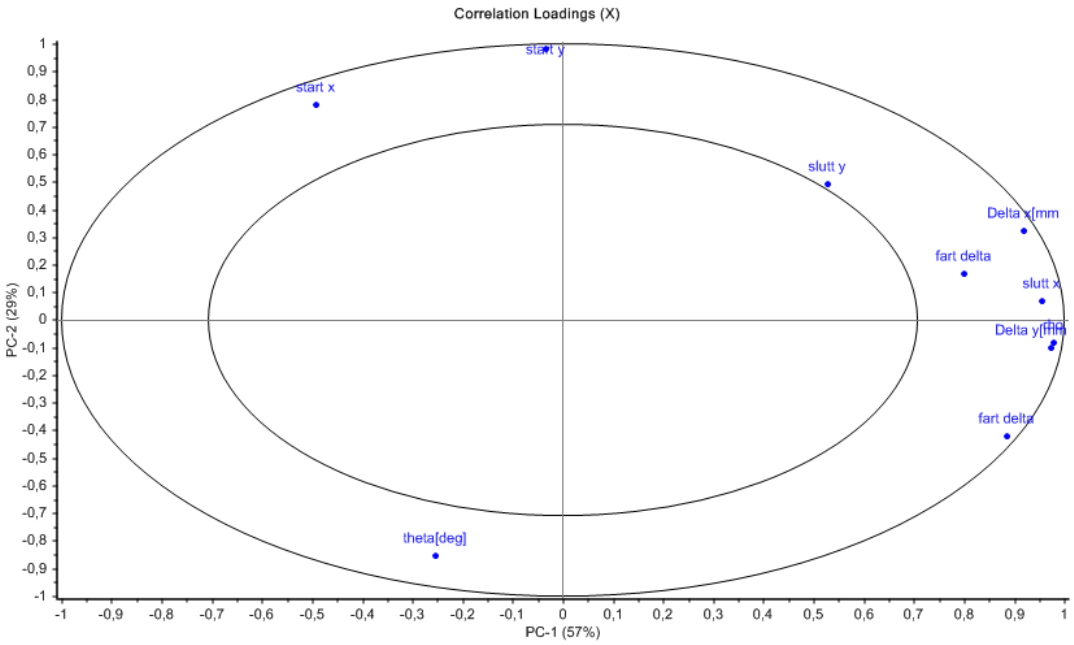

Figure 3.26: PCA correlation loadings plot, for the features calculated for all athletes performing the G4 subtechnique, high intensity

Table 3.13: PCA correlation scores

X correlation	**PC-1**	**PC-2**
Delta x [mm]	0,9187543	0,3211294
Delta y [mm]	0,9727337	-0,1010528
Theta[deg]	-0,2526697	-0,8532013
Rho	0,9782057	-0,08247696
Start x	-0,4913306	0,7794278
Start y	-0,03328302	0,9821457
End x	0,9548216	0,06615718
End y	0,5281578	0,4919672
V_delta CoP X	0,8009251	0,1653242
V_delta CoP Y	0,8850531	-0,4196497

Chapter 4

Discussion

4.1 Phase detection

4.1.1 Cycle detection

The project seemed promising as the raw data showed visually recognizable repeating patterns. The patterns were however expected as recorded data consisted of cyclic movements collected in a very stable lab-environment. In the beginning, the cycles were detected in a very superficial manner. The cycle detection was not part of the objective, and the importance was somewhat neglected. Each cycle was defined by the "zero-force marks" in the time series in order to suit the first athlete. It worked brilliantly for him, but not as well for the others (figure 4.1). A slightly more reliable cycle detector was therefor implemented. This detector found the smallest force value within a given time series (a time series of an average length of the past cycles). This worked somewhat better, but it was still not able to detect all cycles correctly. The cycle detection problem escalated later on, as the algorithm for phase detection requires that every cycle begins with a reposition phase. In retrospect, this part should have been a bigger priority, or the cycles should have been marked manually as suggested in the project description.

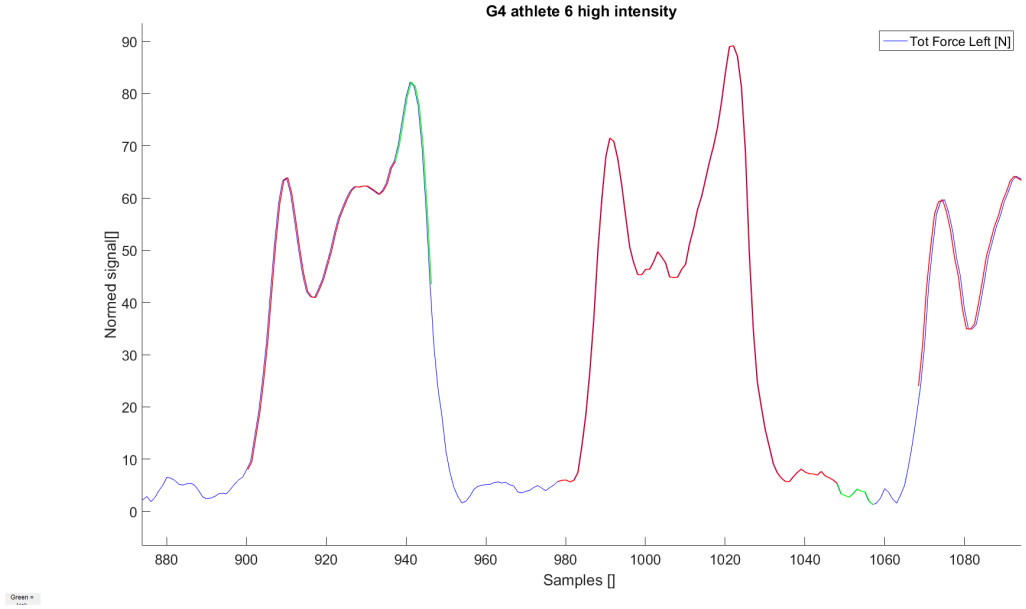

Figure 4.1: Illustration of incorrect phase detection as a consequence of incorrect cycle detection. Green = kick phase, red = gliding phase and blue = reposition phase

4.1.2 Which phases should be included?

It was not possible to detect the moment of the pole plant based on the raw data. In the literature, the pole plant was used in almost all phase definitions. The poling phase was often considered as an individual phase which was highly dependent on the pole plant and liftoff. In order to suit the collected data, three separate phases were included in this thesis: the reposition phase, the gliding phase and the kick phase.

The kick phase was initially a part of the gliding phase (figure 4.2). The different phases needed some clear definition and had to be recognizable in a video. In the search for suitable definitions, the pressure sensors were deemed too inaccurate. There were no clear changes between the phases, only indications as to where they took place. The accelerometer data on the other hand, showed clear changes in the foot movements, and seemed more fitting.

4.1.3 Average data

The averaged data was used in analyzing the different signals in a more understandable plot. It also clarified the main differences between the subtechniques (G2, G3, G4). Some

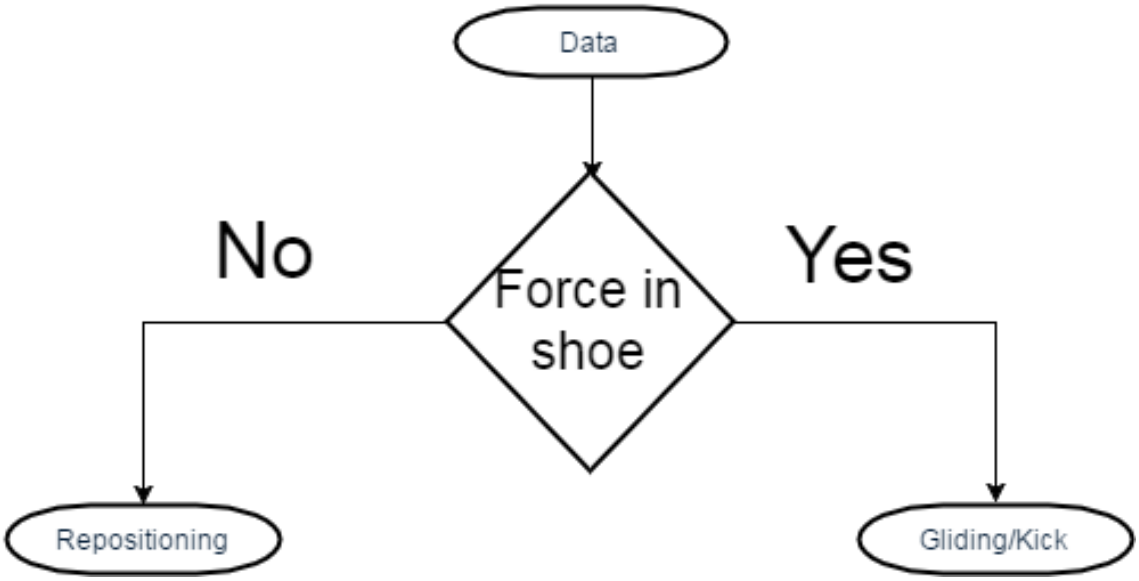

Figure 4.2: Initial phase definitions

signals were the same in all subtechniques, some were not. The acc-x and acc-y signals had consistent hallmarks, common for all subtechniques. The acc-z signal varied a little in the magnitude but not in shape. G4 and G3 had similar foot balance, but the foot balance in the G2 subtechnique differed from the others. In G2 the athlete had very little pressure in the heel throughout the movement. This analysis implied one subtechniques should be emphasized, as an algorithm developed for one technique might not work for another. On the other hand, the analysis gave some insight as to which parameters could work for all subtechniques for use in a future project.

4.1.4 Biomechanical analysis and change features

The biomechanical analysis revealed the signals that actually described the change in the phases. Although the acc-x signal seemed like a good indication for the gliding phase starting point, it was actually later on revealed to describe an earlier sequence in the foot path. The main results of the analysis stated that the acc-z signal could be used to describe the changes. This signal was shown by the average data analysis not to be consistent for all subtechniques, but it was the only signal that explained the point of change between subtechniques exactly. Another approach could have been to estimate the changes based on other features in the data (e.g. that the peak values of the acc-x and acc-y variables indicate that a change is about to happen), and than use a threshold

in total force to set the point. This method was deemed more inaccurate, but would have been more applicable to all subtechniques. Given that the objective gave room for emphasizing one subtechnique, the acc-z approach was chosen.

The gliding phase started with an acceleration in the z-direction at the time of the foot plant. The transition to the kick phase could be described by a positive acceleration in the superior direction of the foot, due to the athletes' slight weight change prior to the kick phase. The transition between the kick phase and the reposition phase was defined by the foot liftoff, and the associated acc-z change. These were all features that could be recognized in a video, and were all possible to implement. The acc-z changes were also possible to detect in the snow recordings.

4.1.5 Phase definitions

A biomechanical analysis was done in order to identify features characteristics of the "phase-changes". The phases were defined by the changes in acc-z values within given time frames. The overall problem was to divide one cycle into phases. Given a correct cycle detection (as discussed in section 4.1.1) the first time sample should be the beginning of the reposition phase. The pressure data was used for localizing the search areas for the extremal points, whereas the acceleration data was used for the detection of the changes.

In order to improve these phase definitions, the search areas could have been reduced, e.g. the gliding phase search area could have started at the peak value of the x-axis accelerometer. This is a known feature that appears in every cycle due to the path of motion, and takes place right before the foot plant (see figure 3.8). Another improvement could have been to require several correlated parameters when detecting each change (e.g. in the start of the kick phase the CoP should not be in the heel).

4.1.6 Phase detection and resulting phase time

The developed algorithm works if the cycles are perfectly divided, with the reposition phase at the beginning. As it does not check whether or not the first time sample actually is a part of the reposition phase, the algorithm fails tremendously if the cycle detection is incorrect. This could be avoided if the algorithm first assures that given features from the repositioning phase is present (e.g. that there was little toe, heel or mid foot force,

which is characteristic for this phase). This could have been implemented rather easily if this algorithm should have been used further. Although, the most important thing to improve is the cycle detection.

The algorithm worked rather well on all athletes (e.g. figures 3.16 and 5.2). The features identified through the biomechanical analysis were valid for all the athletes, which was to be expected. The most challenging phase-change detection was that of the beginning of the kick phase. The ski plant and lift off are distinct easily detected movements. The slight weight change, and the local minimum that appears before the final kick, is not that easy to detect. This phase could alternatively be defined by a set "time-window" that should appear around the maximum force measured in the sole. This would in turn mean that information regarding individual differences in the amount of time spent on the kick phase, would be lost. In the event of further investigation, the importance of this lost information should be discussed with a cross-country specialist.

The statistics presented that the CT on average was 1.58 seconds with a standard deviation of 0.1 seconds for the G4 subtechnique. The G4 gliding phase lasted 0.79 seconds on average, the kick phase 0.15 seconds and the reposition phase 0.57 seconds. At the beginning of athlete 1's G4 high intensity interval, phase times were visually detected from video footage as shown in table 4.1. According to the data the kick phases tend to differ the most from the average compared to the other phases. The kick phase had a longer duration in the video footage than what was calculated by the algorithm. Most likely this was due to inaccurate visual detection, or it might be because the acc-z value (change feature) appeared later than the kick phase actually began. This needs to be investigated further in a future project.

Table 4.1: Statistics from video analysis, G4, high intensity

	Gliding phase [s]	**Kick phase** [s]	**Reposition phase**[s]	**End**
Time	05:29:443	05:30:315	05:30:494	05:31:101
Time of each phase [s]	0.872	0.179	0.607	
% of the cycle	0.53	0.10	0.36	

CT [s]	1.657

Table 4.2: Statistics from video analysis, G2, high intensity

	Gliding phase [s]	**Kick phase** [s]	**Reposition phase**[s]	**End**
Time	11:17:047	11:17:585	11:17:749	11:18:225
Time of each phase [s]	0.538	0.164	0.446	
% of the cycle	0.46	0.14	0.40	

CT [s]	1.178

The average kick phase was longer in the G2 subtechnique than it was in G4, at the expense of the gliding phase. The average CT was shorter for the G2 subtechnique than the G4, with a 0.23 seconds difference on average. The video analysis (table 4.2) showed the same results as the detected difference between these subtechniques.

In a study published in 2016 the CT was calculated to 1.69 seconds with a standard deviation of 0.1 seconds when performing the G4 subtechnique on a treadmill ([Losnegard et al., 2016]). This number is similar to the CTs calculated in this thesis. In the mentioned article the phases were defined as: "poling phase", "reposition phase" and "kick phase", which makes the phase calculations incomparable to our own. Comparison between studies in this field is often a challenge as phase definitions tend to vary between studies.

One of the most important discoveries in this project was the difference in gliding time between the elite and intermediate athletes. This became particularly clear when assessing the percentage of a cycle occupied by the gliding phase. Performing the G4 subtechnique the elite athletes spent an average of 56% of the cycle time on the gliding phase, whereas the intermediate group only spent 44% on the same phase. The G2 subtechnique study showed similar results, 51% for the elite group and 43% for the intermediate group (figure 4.3). This indicates that long gliding phases should be a desirable trait.

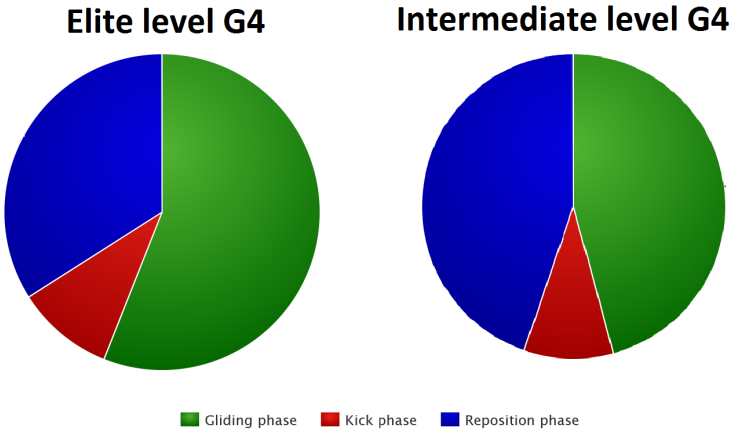

Figure 4.3: Difference in percentage of time spent in the phases during G4. Green = gliding phase, red = kick phase and blue = reposition phase

4.2 Change in CoP during the gliding phase

All athletes changed their CoP in a medial and anterior direction during the gliding phase, in both G2 and G4 subtechniques. The main differences were the CoP starting point and the extent of which the CoP changed in each direction. A similar pattern was also found in the push off in diagonal stride, were the athlete had the highest pressure on the medial forefoot during the kick off phase [Andersson, 2013].

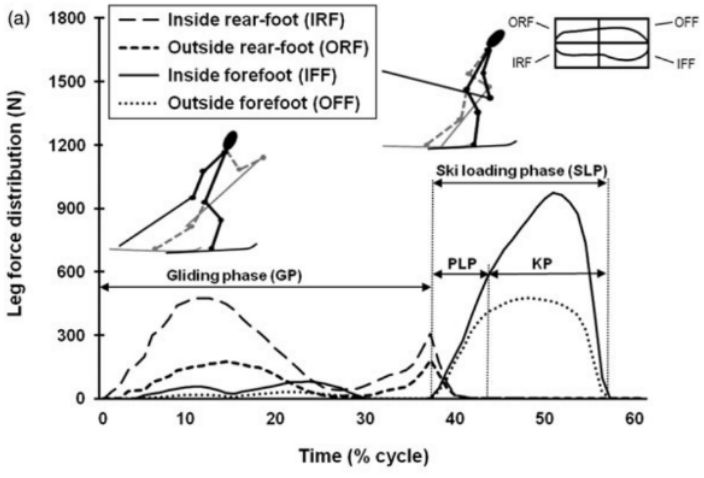

((a)) CoP change during a diagonal skiing cycle [Andersson, 2013]

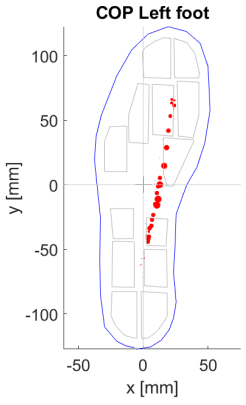

((b)) CoP change during the gliding phase found in this study

Figure 4.4: Similar results found in the kick phase in diagonal stride and G4 skating

Features describing the CoP changes during the gliding phase and the kick phase were extracted. The initial results showed that the kick phase features did not describe the change as well as the gliding phase features did. The gliding phase was therefore prioritized. The most obvious features to be included were the delta x and delta y. They were included in order to distinguish between which athletes had a big change in CoP and which athletes did not. Since the shape of the CoP vector through the gliding phase was so distinct, a polar representation was included. The polar representation is equivalent to the delta x and delta y features, but it might make the visual detection of differences between athletes easier. Redundant features cause unnecessary noise, and should ideally not be included in an automatic classification. Both features were included in the cluster classification, but were manually introduced/removed one-by-one, and did not interfere with the classification result in this study. The distinct start and stop locations were later included as features, as well as the speed of the CoP change. Several other features could have been included, some might even have classified the athletes better. One feature that might be interesting to investigate further is the relative duration (percentage of the cycle) of each phase.

Figures 3.20 and 3.25 showed that it was possible to detect some differences between the two athlete groups. The statistical material was too limited for drawing a statistically significant conclusion, but it implied that the difference in CoP during the gliding phase could vary according to skill level. In order to test this hypothesis a clustering classification was done. This algorithm classified five out of six athletes correctly (figure 4.5). Athlete 3 was misclassified as an elite skier in both G4 and G2 subtechniques, but the other athletes were classified according to their skill levels. Athlete 3's features were more similar to the features of the elite group than to those of the intermediate group, which indicates that athlete 3's technique characteristics are similar to those of the elite athletes.

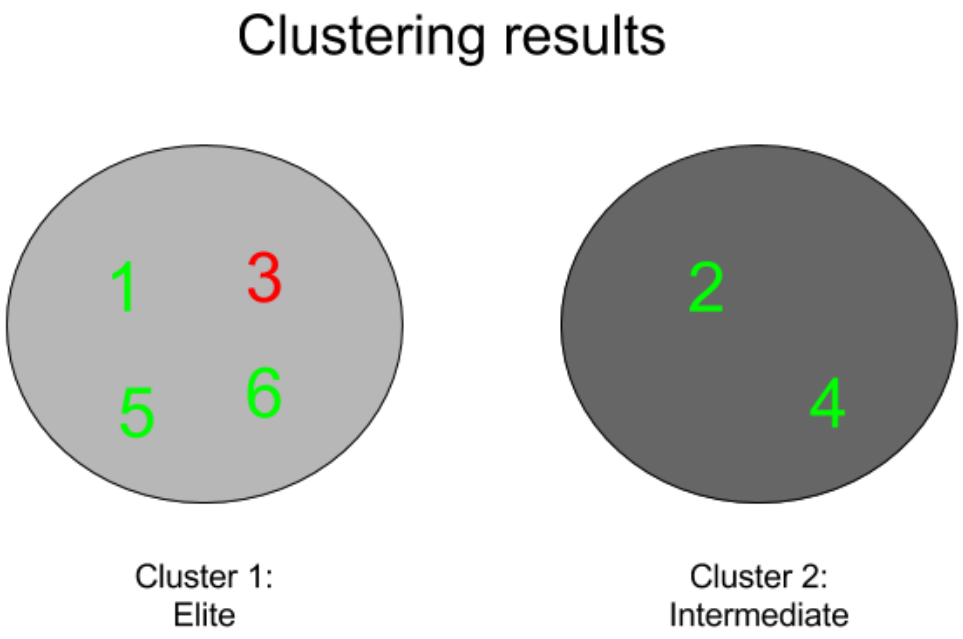

Figure 4.5: Clustering results. Green numbers indicate correct cluster, while red numbers indicate wrong cluster.

4.2.1 PCA

A PCA was performed in order to analyze the features' ability to describe the data regardless of the athletes skill levels. The analysis showed that the delta y, Rho, End x and Start y were the features containing the most information. This is useful information, in the case of future re-investigation. As presented in the introduction the insoles had some inaccuracies regarding medio-lateral measurments, which should be taken into account when choosing features to be included in future studies (i.e. the y-variables is more accurate).

4.3 Future work

The results in this thesis suggests the following topics for future work:

- Implementing a better cycle detection
- Specifying the search areas more precisely

- Implementing more demands for each phase change
- Kick phase definitions
- Implementing and evaluating more features

It should also be evaluated if the implemented phase detection algorithm has enough potential with the suggested improvements, or if the phase detection should be replaced by more refined methods such as a similarity transformation or a Hilbert Huang transform. These methods both need a set of collected templates of each phase to match upon new data. This is a time consuming challenge, and the end result is not guaranteed to be a better fit for the objectives.

Chapter 5

Conclusion

This study has developed a method for dividing a cycle into phases and calculating the time frame for each phase through data from Motion's OpenGo insoles. The phase detection was implemented for subtechniques G2, G3 and G4, with emphasis on G4 as there were some difference in the data between the subtechniques. The main weakness of the phase detection algorithm developed was the dependency of a correct cycle detection and kick phase detection.

An important discovery was that the elite athletes trend towards using a larger percentage of their cycle in the gliding phase than do the intermediate athletes. The CoP changes during the gliding phase and kick phase, have been analyzed. Features from the G4 and the G2 subtechniques during the gliding phase have been extracted. The features were compared between athletes on different skill levels. Calculated features within the elite and intermediate groups respectively indicated that distinction between the classes was possible. This suggests that it might be possible to classify a technique as an elite or intermediate level technique based on the relative amount of time spent in the gliding phase, and the change of CoP during this phase. This indicated that there might be an optimal way of shifting the center of pressure throughout the gliding phase. As the research material in this study was limited to only six subjects, statistically significant conclusions could not be made. Further research is recommended.

The thesis' main contributions are:

1. Phase detection algorithm
2. Analysis of CoP change during the gliding phase and the kick phase

3. Parameters (including time spent in each phase) which describe the different phases
4. Features which describe the CoP change during the gliding phase
5. Features which distinguish between athletes on different skill levels

5.1 Personal evaluation

Being an active person myself I have always had an interest for athletics. Combining this interest with my Cybernetics education has been a fun challenge. It has been exciting to continue the work from the pre-project, and now to present these new discoveries. The thesis had a very wide definition, but I think I managed to limit the objectives in a suitable way. The objectives generated enough work for one more master thesis. On of the biggest challenges I faced, was to figure out how to limit the thesis without loosing important results. Working on this thesis has been very time consuming and challenging. In retrospect I'm satisfied with the work I have done, although I would have liked to study the subject further. There are so many things left to investigate! Even though I leave NTNU wistfully, I also feel ready to start my professional career and face new challenges!

Bibliography

[Alyse L. Kehler and Kram, 2014] Alyse L. Kehler, Eliska Hajkova, H.-C. H. and Kram, R. (2014). Forces and mechanical energy fluctuations during diagonal stride roller skiing; running on wheels? *The Journal of Experimental Biology*, (217):3779–3785.

[Andersson, 2016] Andersson, E. (2016). Physiological and biomechanical factors determining corss-country skiing performance. PhD Thesis, Department of Health Sciences, Mid Sweden University, Sweden.

[Andersson, 2013] Andersson, E., P. B. S. O.-S. T. . H. H. C. (2013). The effects of skiing velocity on mechanical aspects of diagonal cross-country skiing. *Sports Biomechanics*, (13):267–284.

[Andersson, 2014] Andersson, E., S. T. P. B.-S. O. E. G. . H. H. C. (2014). Biomechanical analysis of the herringbone technique as employed by elite crosscountry skiers. *Scandinavian journal of medicine science in sports*, (24):542–552.

[Cline and Dhillon, 2006] Cline, A. K. and Dhillon, I. S. (2006). *Computation of the Singular Value Decomposition*. CRC Press.

[Garsjø, 2016] Garsjø, L. (2016). Automated movement based classification of techniques in classic cross-country skiing. Technical report, NTNU.

[Göpfert, 2013] Göpfert, C., H. H. C. S.-T. M. E. . L. S. J. (2013). Biomechanical characteristics and speed adaptation during kick double poling on roller skis in elite cross-country skiers. *Sports Biomechanics*, (12):154–174.

[Holmberg, 2005] Holmberg, H.C., L. S. S. T.-E. E. . M. (2005). Biomechanical analysis of double poling in elite cross-country skiers. *Med Sci 63 Sports Exerc*, (37):807–818.

[J. Bailey, 2016] J. Bailey, L.Khan, T. G. J. H. . R. W. (2016). *Advances in knowledge discovery and data mining*. Springer.

[Krüger and Edelmann-Nusser, 2010] Krüger, A. and Edelmann-Nusser, J. (2010). Application of a full body inertial measurement system in alpine skiing: a comparison with an optical video based system. *J Appl Biomech*, 26(4):516–521.

[Levy, 2011] Levy, M., E. L. E. N. . R. (2011). Peak force and propulsive impulse comparisons with the diagonal stride during on-snow and roller-skiing. *GISB*.

[Lewicki, 2006] Lewicki, T. H. . P. (2006). *Statistics, methods and application*. StatSoft.

[Lindinger, 2009] Lindinger, S.J., G. C. S. T. M. E. . H. H. (2009). Biomechanical pole and leg characteristics during uphill diagonal roller skiing. *Sports Biomech*, (8):318–333.

[Lindinger SJ, 2009] Lindinger SJ, Stöggl T, M. E. H. H. (2009). Control of speed during the double poling technique performed by elite cross-country skiers. *Med Sci Sports Exerc*, (41):210–220.

[Losnegard et al., 2016] Losnegard, T., Myklebust, H., Ehrhardt, A., and Halln, J. (2016). Kinematical analysis of the v2 ski skating technique: A longitudinal study. *Journal of Sports Sciences*, 0(0):1–9. PMID: 27686117.

[Marsland et al., 2012] Marsland, F., Lyons, K., Anson, J., Waddington, G., Macintosh, C., and Chapman, D. (2012). Identification of cross-country skiing movement patterns using micro-sensors. *Sensors (Basel)*, 12(4):5047–5066.

[MathWorks, 2016] MathWorks (2016). designfilt,design digital filters. [Online; accessed 15.02.2016].

[Meland, 2016] Meland, H. (2016). A study of published methods, and implementation and critique of a markov-chain classifier, for classification of cross-country skiing techniques. Technical report, NTNU.

[Moticon, 2017] Moticon (2017). [Online: accessed 03.01.17].

[Myklebust, 2016] Myklebust, H. (2016). *Quantification of movement patterns in cross-country skiing using inertial measurement units.* PhD thesis, THE NORWEGIAN SCHOOL OF SPORT SCIENCES.

[Myklebust et al., 2014] Myklebust, H., Losnegard, T., and Hallen, J. (2014). Differences in V1 and V2 ski skating techniques described by accelerometers. *Scand J Med Sci Sports*, 24(6):882–893.

[Novel.de, 2017] Novel.de (2017). The pedar system - the quality in-shoe dynamic pressure measuring system. [Online: accessed 03.01.17].

[Oppenheim and Buck, 1999] Oppenheim, Alan V., R. W. S. and Buck, J. R. (1999). *Discrete-Time Signal Processing 2nd Ed.* Upper Saddle River Prentice Hall.

[Orfanidis, 2010] Orfanidis, S. J. (2010). *Introduction to Signal Processing.* Pearson Education, Inc.

[Rahmati et al., 2014] Rahmati, H Aamo, O. M., Stavdahl, Ø., Dragon, R., and Adde, L. (2014). Video-based early cerebral palsy prediction using motion segmentation. 2014:3779–3783.

[Sakurai et al., 2014] Sakurai, Y., Fujita, Z., and Ishige, Y. (2014). Automated identification and evaluation of subtechniques in classical-style roller skiing. *J Sports Sci Med*, 13(3):651–657.

[Sakurai et al., 2016] Sakurai, Y., Fujita, Z., and Ishige, Y. (2016). Automatic identification of subtechniques in skating-style roller skiing using inertial sensors. *Sensors*, 16(4):473.

[Stöggl, 2014] Stöggl, T., . H. (2014). Three-dimensional force and kinematic interactions in v1 skating at high speeds. *Medicine Science in Sports Exercise*, pages 1232–1242.

[Stöggl and Lindinger, 2008] Stöggl, Thomas, E. M. and Lindinger, S. (2008). Biomechanical comparison of the double-push technique and the conventional skate skiing technique in cross-country sprint skiing. *Journal of sports sciences 26.11*, pages 1225–1233.

[Stöggl, 2009] Stöggl, T., M. E. A. M. . H. (2009). General strength and kinetics: fundamental to sprinting faster in cross country skiing? *Scand J Med Sci Sports*, pages 791–803.

[Stöggl et al., 2014] Stöggl, T., Holst, A., Jonasson, A., Andersson, E., Wunsch, T., Norström, C., and Holmberg, H. C. (2014). Automatic classification of the sub-techniques (gears) used in cross-country ski skating employing a mobile phone. *Sensors (Basel)*, 14(11):20589–20601.

[Stöggl T, 2010] Stöggl T, Kampel W, M. E. L. S. (2010). Double-push skating versus v2 and v1 skating on uphill terrain in cross-country skiing. *Med Sci Sports Exerc*, pages 187–196.

[Stggl and Martiner, 2017] Stggl, T. and Martiner, A. (2017). Validation of moticons opengo sensor insoles during gait, jumps, balance and cross-country skiing specific imitation movements. *Journal of Sports Sciences*, 35(2):196–206. PMID: 27010531.

[Våga, 2008] Våga, S. (2008). Identifikasjon av menneskelig aktivitet basert på kroppsmonterte sensorer.

Appendix

Table 5.1: Calculated time's of each phase for athlete 1 in G4 high speed.

Cycle #	**Cycle time [s]**	**Gliding phase [s]**	**Kick phase [s]**	**Reposition phase [s]**
1	1,70	0,98	0,14	0,98
2	1,61	0,94	0,12	0,94
3	1,55	0,72	0,12	0,72
4	1,67	0,82	0,14	0,82
5	1,54	0,82	0,22	0,82
6	1,45	0,68	0,14	0,68
7	1,57	0,6	0,22	0,6
8	1,71	0,6	0,18	0,88
9	1,42	0,88	0,12	0,82
10	1,53	0,82	0,12	0,96
11	1,75	0,96	0,28	0,70
12	1,42	0,7	0,14	0,94
13	1,53	0,94	0,16	0,78
14	1,75	0,78	0,18	0,72
15	1,56	0,72	0,16	0,74
16	1,45	0,74	0,18	0,80
17	1,57	0,80	0,12	0,92
18	1,33	0,92	0,14	0,82
19	1,48	0,82	0,14	0,86
20	1,46	0,86	0,16	0,74
21	1,53	0,74	0,16	0,72
22	1,67	0,72	0,24	0,62
Average:	**1,55**	**0,78**	**0,16**	**0,55**
% of a cycle		**0,50**	**0,11**	**0,36**

Table 5.2: Calculated time's of each phase for athlete 2 in G4 high speed.

Cycle #	**Cycle time [s]**	**Gliding phase [s]**	**Kick phase [s]**	**Reposition phase [s]**
1	1,74	0,72	0,18	0,84
2	1,71	0,82	0,16	0,73
3	1,68	0,78	0,20	0,70
4	1,67	0,72	0,16	0,79
5	1,83	0,82	0,22	0,79
6	1,46	0,62	0,20	0,64
7	1,66	0,68	0,24	0,74
8	1,82	0,80	0,14	0,88
9	1,68	0,62	0,22	0,84
10	1,68	0,90	0,16	0,62
11	1,60	0,66	0,22	0,72
12	1,60	0,62	0,14	0,84
13	1,54	0,60	0,16	0,78
14	1,65	0,74	0,14	0,77
15	1,51	0,66	0,18	0,67
16	1,33	0,54	0,24	0,55
17	1,37	0,72	0,14	0,51
18	1,53	0,68	0,16	0,69
19	1,68	0,66	0,16	0,86
20	1,65	0,58	0,26	0,81
21	1,53	0,66	0,24	0,63
22	1,42	0,64	0,22	0,56
Average:	**1,60**	**0,64**	**0,18**	**0,69**
% of a cycle		**0,40**	**0,11**	**0,43**

Table 5.3: Calculated time's of each phase for athlete 3 in G4 high speed.

Cycle #	**Cycle time [s]**	**Gliding phase [s]**	**Kick phase [s]**	**Reposition phase [s]**
1	1,88	1,04	0,16	0,68
2	1,86	1,08	0,12	0,66
3	1,63	0,86	0,14	0,63
4	1,49	0,68	0,12	0,69
5	1,77	0,80	0,18	0,79
6	1,84	0,88	0,16	0,81
7	1,71	0,72	0,14	0,85
8	1,91	1,08	0,12	0,71
9	1,70	0,98	0,12	0,60
10	1,98	1,36	0,12	0,50
11	1,65	0,68	0,14	0,83
12	1,84	0,86	0,20	0,78
13	1,75	0,90	0,14	0,70
14	1,70	0,74	0,14	0,83
15	1,68	0,72	0,12	0,84
16	1,62	0,78	0,14	0,70
17	1,78	0,74	0,14	0,89
18	1,72	0,78	0,12	0,82
19	1,52	0,76	0,12	0,64
20	1,73	0,74	0,14	0,85
21	1,75	0,70	0,24	0,81
22	1,63	0,76	0,14	0,73
Average:	**1,72**	**0,78**	**0,14**	**0,70**
% of a cycle		**0,45**	**0,08**	**0,41**

Table 5.4: Calculated time's of each phase for athlete 4 in G4 high speed.

Cycle #	**Cycle time [s]**	**Gliding phase [s]**	**Kick phase [s]**	**Reposition phase [s]**
1	1,56	0,80	0,14	0,62
2	1,38	0,64	0,14	0,60
3	1,49	0,90	0,14	0,46
4	1,49	0,70	0,18	0,62
5	1,50	1,04	0,14	0,32
6	1,40	0,78	0,14	0,48
7	1,36	0,74	0,14	0,48
8	1,29	0,64	0,16	0,49
9	1,54	0,76	0,12	0,65
10	1,38	0,66	0,16	0,56
11	1,48	0,96	0,14	0,38
12	1,32	0,78	0,14	0,40
13	1,44	0,88	0,18	0,38
14	1,46	0,72	0,14	0,59
15	1,36	0,68	0,16	0,52
16	1,45	0,74	0,12	0,59
17	1,37	0,82	0,14	0,41
18	1,57	1,04	0,16	0,37
19	1,46	0,60	0,18	0,67
20	1,43	0,78	0,16	0,49
21	1,39	0,78	0,16	0,45
22	1,45	0,68	0,14	0,63
Average:	**1,43**	**0,70**	**0,14**	**0,52**
% of a cycle		**0,49**	**0,10**	**0,36**

Table 5.5: Calculated time's of each phase for athlete 5 in G4 high speed.

Cycle #	**Cycle time [s]**	**Gliding phase [s]**	**Kick phase [s]**	**Reposition phase [s]**
1	1,34	0,72	0,16	0,46
2	1,51	0,78	0,18	0,55
3	1,55	0,80	0,18	0,57
4	1,47	0,88	0,16	0,43
5	1,51	0,68	0,14	0,69
6	1,75	1,56	0,06	0,14
7	1,32	0,74	0,16	0,42
8	1,42	0,82	0,18	0,43
9	1,50	0,86	0,12	0,52
10	1,32	0,64	0,12	0,56
11	1,52	0,70	0,16	0,65
12	1,51	0,68	0,18	0,65
13	1,82	1,58	0,10	0,14
14	1,19	0,70	0,16	0,33
15	1,62	0,74	0,16	0,72
16	1,51	0,88	0,14	0,48
17	1,58	0,78	0,18	0,63
18	1,89	1,36	0,10	0,43
19	1,26	0,74	0,16	0,36
20	1,47	0,78	0,16	0,53
21	1,65	0,82	0,16	0,67
22	1,57	0,76	0,18	0,63
Average:	**1,54**	**0,82**	**0,14**	**0,49**
% of a cycle		**0,53**	**0,09**	**0,32**

Table 5.6: Calculated time's of each phase for athlete 6 in G4 high speed.

Cycle #	**Cycle time [s]**	**Gliding phase [s]**	**Kick phase [s]**	**Reposition phase [s]**
1	1,94	1,20	0,12	0,62
2	1,63	1,24	0,10	0,29
3	2,63	2,10	0,16	0,37
4	1,63	0,68	0,14	0,81
5	1,50	0,68	0,16	0,66
6	1,91	1,16	0,24	0,51
7	1,67	1,22	0,16	0,29
8	1,74	1,28	0,14	0,32
9	1,15	0,66	0,14	0,35
10	1,69	0,64	0,18	0,87
11	1,55	0,74	0,18	0,63
12	2,04	1,40	0,18	0,46
13	1,62	1,30	0,10	0,22
14	1,43	1,02	0,10	0,31
15	1,74	0,98	0,10	0,66
16	1,38	0,78	0,18	0,42
17	1,61	0,86	0,14	0,61
18	1,63	0,76	0,18	0,69
19	1,62	0,82	0,14	0,66
20	1,62	0,72	0,18	0,72
21	2,18	1,38	0,08	0,72
22	1,55	1,40	0,08	0,07
Average:	**1,67**	**1,04**	**0,12**	**0,41**
% of a cycle		**0,62**	**0,07**	**0,24**

Table 5.7: Calculated time's of each phase for athlete 2 in G2 high speed.

Cycle #	**Cycle time [s]**	**Gliding phase [s]**	**Kick phase [s]**	**Reposition phase[s]**
1	2.00	0.92	0.16	0.92
2	2.00	0.92	0.18	0.90
3	1.92	0.90	0.20	0.82
4	2.12	1.06	0.24	0.82
5	1.92	0.90	0.18	0.84
6	1.71	0.78	0.16	0.77
7	1.89	0.78	0.22	0.89
8	1.97	0.94	0.24	0.79
9	1.85	0.96	0.20	0.69
10	1.84	0.94	0.20	0.70

	Mean	**Std**	**Mean**	**Std**	**Mean**	**Std**	**Mean**	**Std**
Average time [s]	1.87	0,51	0.80	0.24	0.18	0.06	0.74	0,23
Average % of a cycle			0,43		0,09		0,39	

Table 5.8: Calculated time's of each phase for athlete 3 in G2 high speed.

Cycle #	**Cycle time [s]**	**Gliding phase [s]**	**Kick phase [s]**	**Reposition phase[s]**
1	1.30	0.54	0.12	0.64
2	1.39	0.52	0.14	0.73
3	1.29	0.54	0.14	0.61
4	1.42	0.50	0.16	0.76
5	1.23	0.54	0.14	0.55
6	1.32	0.52	0.14	0.66
7	1.46	0.56	0.16	0.74
8	1.19	0.50	0.14	0.55
9	1.28	0.52	0.12	0.64
10	1.44	0.54	0.12	0.78

	Mean	**Std**	**Mean**	**Std**	**Mean**	**Std**	**Mean**	**Std**
Average time [s]	1.33	0,28	0.51	0.12	0.14	0.04	0.62	0,16
Average % of a cycle			0,39		0,10		0,46	

Table 5.9: Calculated time's of each phase for athlete 4 in G2 high speed.

Cycle #	**Cycle time [s]**	**Gliding phase [s]**	**Kick phase [s]**	**Reposition phase[s]**
1	1.34	0.64	0.22	0.48
2	1.25	0.54	0.20	0.51
3	1.38	0.70	0.18	0.50
4	1.32	0.66	0.20	0.46
5	1.22	0.70	0.18	0.34
6	1.21	0.42	0.20	0.59
7	1.36	0.74	0.18	0.44
8	1.29	0.56	0.20	0.53
9	1.30	0.62	0.20	0.48
10	1.25	0.60	0.16	0.49

	Mean	**Std**	**Mean**	**Std**	**Mean**	**Std**	**Mean**	**Std**
Average time [s]	1.36	0,33	0.66	0.22	0.18	0.05	0.46	0,15
Average % of a cycle			0,48		0,13		0,34	

Table 5.10: Calculated time's of each phase for athlete 5 in G2 high speed.

Cycle #	**Cycle time [s]**	**Gliding phase [s]**	**Kick phase [s]**	**Reposition phase[s]**
1	1.30	0.62	0.16	0.52
2	1.22	0.64	0.16	0.42
3	1.34	0.58	0.16	0.60
4	1.28	0.60	0.18	0.50
5	1.28	0.58	0.14	0.56
6	1.40	0.88	0.22	0.30
7	1.28	0.58	0.18	0.52
8	1.32	0.54	0.24	0.54
9	1.14	0.62	0.16	0.36
10	1.36	0.96	0.14	0.26

	Mean	**Std**	**Mean**	**Std**	**Mean**	**Std**	**Mean**	**Std**
Average time [s]	1.33	0,34	0.64	0.27	0.16	0.04	0.46	0,16
Average % of a cycle			0,48		0,12		0,35	

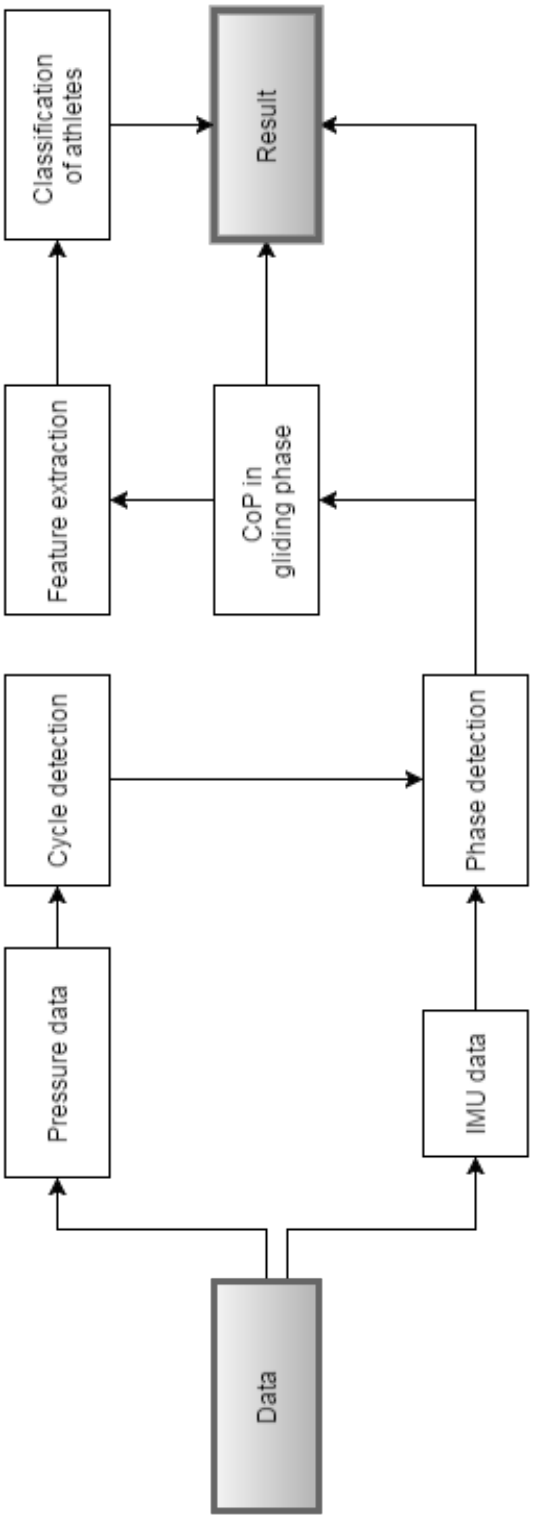

Figure 5.1: Data flow

Table 5.11: Calculated time's of each phase for athlete 6 in G2 high speed.

Cycle #	Cycle time [s]	Gliding phase [s]	Kick phase [s]	Reposition phase[s]
1	2.42	2.02	0.14	0.26
2	2.35	1.74	0.18	0.43
3	2.43	1.64	0.16	0.63
4	2.48	1.86	0.14	0.48
5	2.41	1.64	0.16	0.61
6	2.26	1.72	0.16	0.38
7	1.25	0.56	0.18	0.51
8	1.19	0.46	0.20	0.53
9	2.37	1.68	0.16	0.53
10	1.18	0.56	0.16	0.46

	Mean	Std	Mean	Std	Mean	Std	Mean	Std
Average time [s]	1,87	0,79	1,14	0.68	0.15	0.05	0.41	0,18
Average % of a cycle			0,61		0,08		0,22	

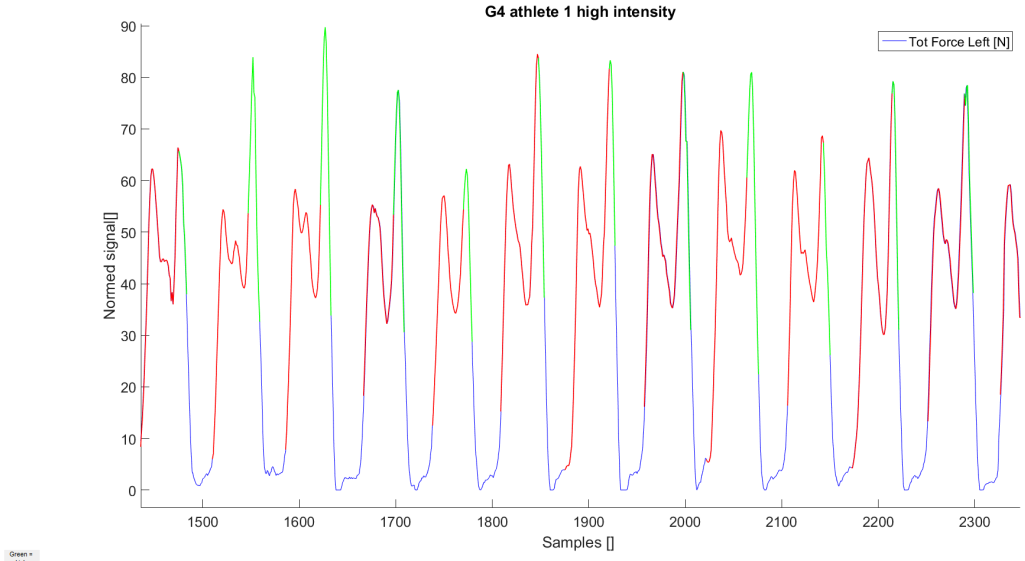

Figure 5.2: Illustration of the phase detection for athlete 2 in G4. Red = gliding phase, blue = reposition phase and green = kick phase.

Table 5.12: Clustering results for G4

Athlete	Delta x[mm]	Delta y[mm]	Theta[deg]	Rho[mm]	Start x[mm]	Start y[mm]	End x[mm]	End y[mm]	V_delta COP X[m/s]	V_delta COP Y[m/s]	Class
1	24,62	121,64	76,38	123,98	0,56	-60,52	12,82	0,88	0,03	0,15	0
2	10,60	67,28	76,73	68,06	1,65	-52,25	8,56	-3,05	0,015	0,09	1
3	20,54	125,30	76,62	126,82	-1,55	-67,70	12,40	27,87	0,02	0,15	0
4	22,77	93,53	73,60	96,27	1,51	-38,88	10,53	12,37	0,02	0,13	1
5	19,16	102,1	75,44	103,77	2,31	-28,82	10,86	32,39	0,02	0,11	0
6	26,51	122,88	74,20	125,49	1,51	-23,99	13,76	40,90	0,02	0,13	0

Table 5.13: Clustering results for G2

Athlete	Delta X [mm]	Delta Y [mm]	Theta [deg]	Rho [mm]	Start X [mm]	Start Y [mm]	End X [mm]	End Y [mm]	V delta COP X [m/s]	V delta COP Y [m/s]	Class
1	10,89	40,34	71,56	41,91	10,24	31,53	13,08	21,88	0,020	0,08	1
2	12,86	77,48077	74,86	78,41662	-0,30	-53,34	6,65	-2,27	0,01	0,08	0
3	10,93	61,87	76,06	62,88	6,72	18,44	11,13	24,96	0,01	0,11	1
4	13,72	73,88182	76,18	75,10	1,31	-36,07	7,656818	7,88	0,01905098	0,10	0
5	18,58	53,07	67,83	56,64	7,22	34,29	9,35	30,37	0,02	0,07	1
6	25,54	78,60	66,60	82,41	8,08	17,2	13	30,41	0,02	0,06	1

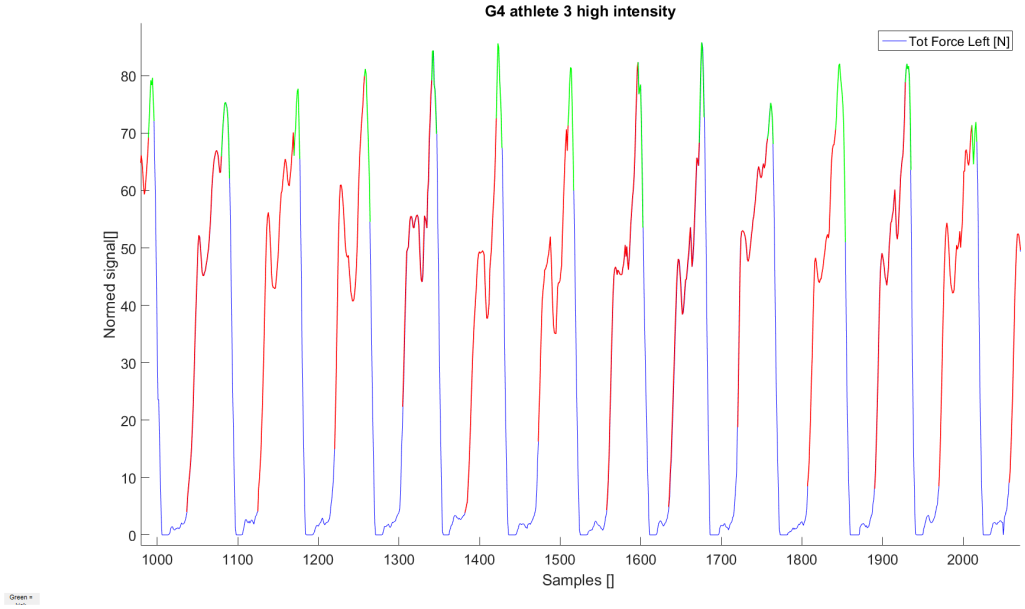

Figure 5.3: Illustration of the phase detection for athlete 3 in G4. Red = gliding phase, blue = reposition phase and green = kick phase.

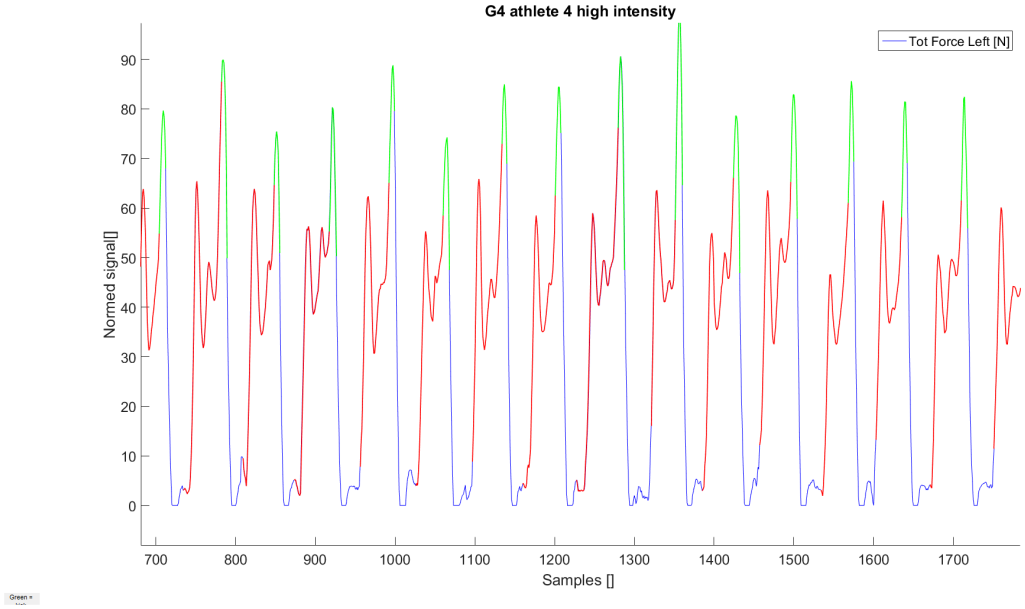

Figure 5.4: Illustration of the phase detection for athlete 4 in G4. Red = gliding phase, blue = reposition phase and green = kick phase.

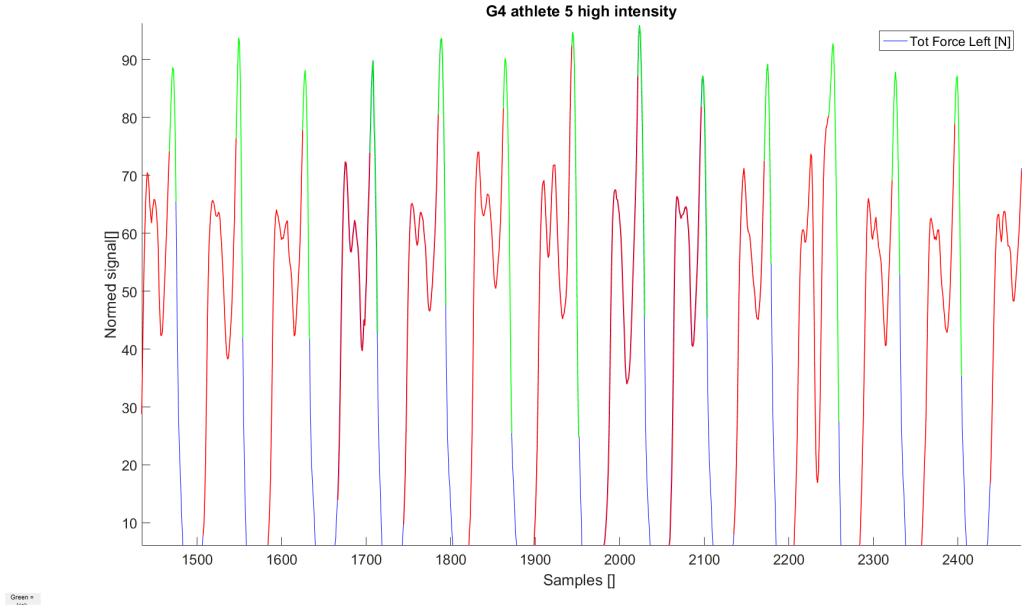

Figure 5.5: Illustration of the phase detection for athlete 5 in G4. Red = gliding phase, blue = reposition phase and green = kick phase.

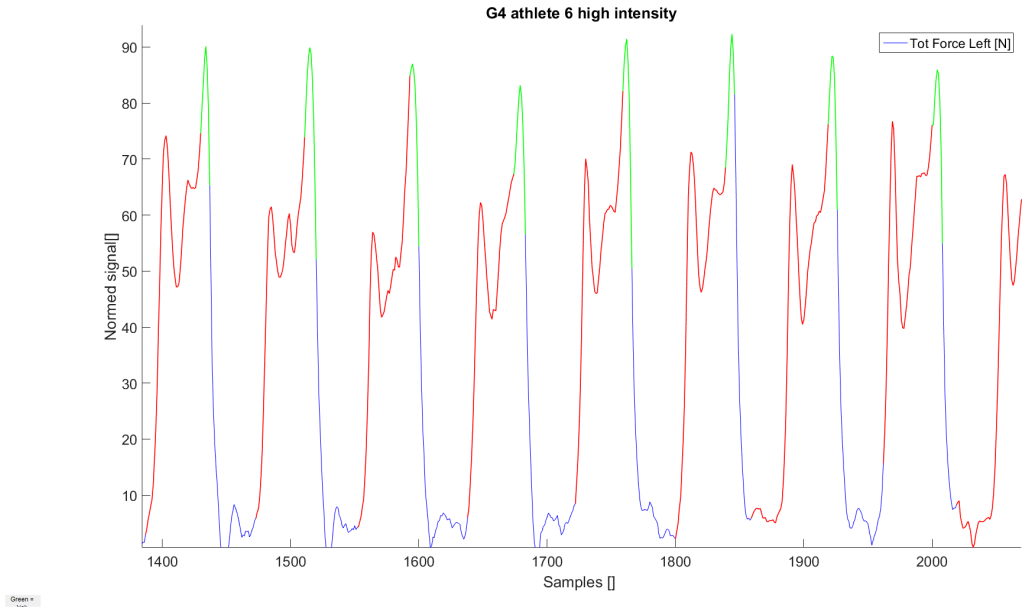

Figure 5.6: Illustration of the phase detection for athlete 6 in G4. Red = gliding phase, blue = reposition phase and green = kick phase.